Semaphorins comprise a large family of phylogenetically conserved soluble and transmembrane molecules that are encoded by a large gene family divided into eight classes[1]. Semaphorins were originally identified as repulsive axon guidance cues involved in induction of growth cone collapse in developing neurons[2-4]. Later studies also found widespread roles in a variety of developmental and pathological conditions[5,6]. Sema4D, a class 4 semaphorin, has facilitated our understanding of how semaphorin signals regulate the cytoskeletal changes that mediate repulsion[7-10]. Sema4D, also known as CD100, induces repulsive changes such as growth cone collapse in cultured hippocampal neurons and retinal ganglion cells[7]. For this repulsion, Sema4D binds to PlexinB1, a member of the plexin family, a predominant group of semaphorin receptors[7]. Both Sema4D and PlexinB1 contain a distinctively conserved Sema domain of ~400 amino acids, featuring a seven-blade β-propeller fold in their respective extracellular domains[1,3]. Sema4D and PlexinB1 interact with each other through their respective Sema domains[5]. In the intracellular region, PlexinB1 has two GTPase activating protein (GAP) domains segmented by a GTPase binding domain and a PDZ-binding site at the C terminal[5,7,8]. Binding of Sema4D to PlexinB1 induces clustering of the PlexinB1 receptors, leading to activation of GAP activities also facilitated by active GTPase and Rnd1-dependent relief of GAP domain interaction[8]. PlexinB1 GAP activity promotes conversion from GTP-bound (active) R-Ras to GDP–bound (inactive) R-Ras, resulting in downregulation of R-Ras activity, which causes a decrease in integrin-based cell adhesion to the extracellular matrix, and subsequently, growth cone collapse in cultured hippocampal neurons[8]. PlexinB1 also allows the intracellular RhoA-specific guanine nucleotide exchange factors (GEF) PDZ-RhoGEF and leukemia-associated RhoGEF (LARG) to bind to the PDZ-binding motif at the C terminal of PlexinB1[7]. Sema4D binding to PlexinB1 stimulates the GEF activities of PDZ-RhoGEF and LARG, promoting conversion from the GDP-bound form to the GTP-bound form of RhoA, a Rho GTPase crucial for the regulation of actin and microtubule dynamics[7]. The increase in GTP-bound RhoA functions to enhance actomyosin contractility through Rho kinase activation and myosin light chain phosphorylation, thereby leading to growth cone collapse of hippocampal neurons[5,7]. Thus, both R-Ras GAP activity and PDZ-RhoGEF-mediated RhoA activation by plexin-B1 are necessary for Sema4D-induced growth cone collapse of cultured hippocampal neurons[7,8].

The crucial roles of Sema4D in growth cone guidance have been demonstrated in many studies using primary neurons in culture, suggesting involvement in the control of neuronal wiring *in vivo*[7-10]. A recent RNAi-based approach revealed that Sema4D is required for GABAergic synapse development in hippocampal neurons[11]. However, direct evidence that Sema4D is actually involved in the development of the functional neuronal network necessary for the regulation of neurobehavioral performance is still lacking. To gain insight into whether Sema4D is involved in the formation of the neuronal networks controlling mouse behavior, we subjected Sema4D-deficient mice to a series of mouse behavioral analyses. The results revealed accelerated motor activities in Sema4D-deficient mice in several of the behavioral tests.

Materials and Methods

Sema4D-deficient mice: Mice deficient in Sema4D were generated by gene targeting of E14.1 embryonic stem (ES) cells[12]. Briefly, targeting vectors were designed to replace the exon containing the initiation codon with a neomycin-resistance gene then introduced into E14.1 Embryonic stem cells using electroporation. Clones resistant to G418 and ganciclovir were screened by PCR and confirmed by Southern blot analysis. Mutant ES cells were injected into blastocysts (C57BL/6) then transferred into the uteri of pseudopregnant mice to generate chimeras. The chimeras were bred with C57BL/6 mice for germline transmission of the mutant allele. Pairs of resultant heterozygous mice were subsequently bred to obtain homozygous Sema4D-deficient mice. The resulting mice were backcrossed with C57BL/6 mice. The present study used F9 generation knockout mice (three to four months old), with their wild-type littermates as controls. The mice were housed in the animal facilities of Wakayama Medical University. The care and sacrifice of animals and the experiment protocols were performed according to the guidelines promulgated by the Physiological Society of Japan and the guidelines on animal experiments of Wakayama Medical University. Our institutional Animal Ethics Review committee approved the experimental protocol.

Immunoblotting: For Western blot analysis, tissue extracts were prepared from mouse brain containing cerebellum. Twenty micrograms of each sample were adjusted to give a final solution of 60 mM Tris-HCl (pH 6.8), 2% SDS, 10% glycerol, 0.1% bromophenol blue and 5% β-mercaptoethanol. This solution was then heated at 100°C for 5 min, electrophoresed through a 10% SDS-polyacrylamide gel, and transferred to polyvinylidine difluoride membranes (Amersham Pharmacia Biotech, Buckinghamshire, UK). Sema4D was detected with CD100 antibody (BD Transduction Laboratories, NJ, USA) using an ECL-plus Western blot detection system in accordance with the manufacturer's instructions (Amersham).

Calbindin-staining: Wild-type (n=4) and Sema4D-deficient littermates (n=5) were anesthetized and perfused intracardially with 4% paraformaldehyde. Four millimeter-thick coronary sections containing cerebellum and brain stem were prepared with the acrylic mouse coronal brain matrices (ROBOZ SURGICAL, Gaithersburg, MD) and post-fixed in 4% paraformaldehyde solution overnight at 4°C. They were then equilibrated in a gradually increasing concentration of sucrose solution (12, 15, 18, 20, 25 and 30%) in PBS at 4°C. Once equilibrated, tissues were mounted in Tissue-Tek O.C.T. compound and cut into 25-μm-thick coronal sections on a cryostat (Leica). To detect calbindin in the cerebellum, tissue sections were treated in 10 mM sodium citrate buffer (pH 6.0) and placed in a microwave oven for antigen unmasking. After blocking, tissue sections were incubated with a rabbit antibody recognizing calbindin (Chemicon International, Temecula, CA, USA) at 4°C overnight. Sections were then incubated with peroxidase-labeled polymer conjugated to goat anti-rabbit immunoglobulin (DakoCytomation, Kyoto, Japan), and Purkinje cells with calbindin were visualized in situ according to the DAB detection procedure. Pictures were taken at a magnification of 400 × using a light microscope equipped with a 3CCD camera (HV-C20S; Nikon, Tokyo, Japan).

Footprint analysis: The footprint test was performed to compare the gait of Sema4D-deficient mice (n=10) with that of wild-type controls (n=10). The hind- and forefeet were coated with black and red nontoxic paint, respectively. The mice were then allowed to walk along a 50-cm-long 10-cm-wide runway covered with a sheet of white paper. Stride length, hind-base width, front-base width and distance from left or right hind footprints were measured following as previously reported[13].

Open-field test: Each mouse was placed in a circular open-field area (diameter: 80 cm) and allowed to freely explore the environment for 20 minutes. The horizontal activities of 19 male wild-type and 18 male Sema4D-deficient mice were measured using a computer-assisted video tracking system (CompACT vas; Muromachi Kikai, Tokyo, Japan).

Home cage locomotor activity: Mice (ten wild-type and eight Sema4D-deficient mice) were individually housed in a standard home cage and acclimated for 48 hours. Home cage activity was monitored over 24 hours using the SUPERMEX system with a passive-type infrared ray sensor (Muromachi Kikai, Tokyo).

Elevated plus-maze test: The elevated plus-maze test was conducted using nine wild-type and eight Sema4D-deficient mice following a previously established method[14]. Time spent in the closed and open arms, and entry into the open and closed arms were measured using a computer-assisted video tracking system (CompACT vas; Muromachi Kikai, Tokyo, Japan).

Light/dark exploration test: The light-dark exploration test was conducted using ten wild-type and eight Sema4D-deficient mice as previously reported[14]. Time spent and full-body transitions into the light compartments, and total full-body transitions between the light and dark compartments were measured by applying a computer-assisted video tracking system (CompACT vas; Muromachi Kikai, Tokyo, Japan).

Prepulse inhibition of the acoustic startle response: Prepulse inhibition of acoustic startle responses was measured using 14 male wild-type and 19 male Sema4D-deficient mice with the SR-Lab System (San Diego Instruments, San Diego, CA, USA) as previously described[15]. A test session was initiated by placing a mouse in the plexiglas cylinder to which it was acclimated for five minutes. A test session was composed of seven trial types. A 40-msec, 120dB sound burst was used as the startle stimulus. The present study used five different acoustic prepulses plus auditory startle stimulus trials. The prepulse sound preceded the onset of the startle stimulus by 100 msec. The 20-msec prepulse sounds were 74, 78, 82, 86, or 90dB. Additionally, in some trials no stimulus was presented to measure base-line movement in the cylinders. Six blocks of seven trial types were presented in a pseudorandom manner such that each trial type was presented once within a block. The mean intertrial interval was set at 15 sec (ranging from 10 to 25 sec). The startle response was recorded for 160 msec (measuring the response every 1 msec) starting with onset of the startle stimulus. The background noise level in each chamber was 69dB. The maximum startle amplitude recorded during the 160-msec sampling window was used as the dependent variable. Percent prepulse inhibition of a startle response was calculated as: 100-[(startle response on acoustic prepulse plus startle stimulus trials/startle response alone trials) x 100]. Acoustic response amplitude data were analyzed using the Student's *t*-test. Prepulse inhibition data were analyzed with two-way (genotype × prepulse sound level) ANOVA with repeated measures.

Adhesive tape removal test: The adhesive tape removal task involved 20 wild-type and 16 Sema4D-deficient mice, and was performed following the protocol described by others[16]. Adhesive tape of five sizes (0.625, 0.5, 0.375, 0.25, 0.125 inches^2) was attached to the forehead in the above order. In response, mice raised both forepaws and attempted to remove the tape. Each trial was given a score equal to the size of the largest tape the mouse was unable to remove within 60 sec (5 to 1, a higher score equals a worse performance). Results represented the average from two trials.

Rotarod test: The rotarod test for motor coordination involved 14 male wild-type and 14 male Sema4D-deficient mice, and was initially performed by placing each mouse on a rotating drum (Ugo Basile; Stoelting, Wood Dale, IL, USA) at 4 rpm. The latency to falling off the drum was measured as an index of motor coordination. After one week, each mouse was again placed on the rotating drum and subjected to acceleration from 4 to 20 rpm over a five-minute period. The latency for remaining on the rotating drum was measured as another parameter of motor coordination.

Water maze analysis: Spatial learning and memory were tested in 17 male wild-type and 18 male Sema4D-deficient mice using a Morris water maze consisting of a circular plastic pool (diameter: 120 cm; depth: 25 cm). The pool was located in a rectangular room (width: 220 cm; length: 260 cm; height: 240 cm) with numerous visual cues. For swimming tracking, a small TV camera was fixed to the end of a metal rod extending over the pool. Mice were trained to locate a hidden escape platform during two-trial daily sessions conducted over 16 days. In each task, the mice were required to locate and climb onto a hidden circular platform (diameter: 11 cm) submerged 1 cm below the surface of opaque water (temperature of 25 ± 1°C). The hidden platform was located at the center of a quadrant of the pool; this position was fixed throughout the task. Mice were allowed to search for the platform for 60 sec, and the time spent reaching the platform (latency) was recorded. During the probe trial on day 17, the platform was removed and each mouse was allowed to search for 60 sec. Both the quadrant search times and platform crossings were measured post-hoc from videotape recordings of the probe trials. The results were evaluated by ANOVA followed by Dunnett's test for comparison between wild-type and Sema4D-deficient mice.

Novel object recognition test: The object recognition test was performed according to a modified previously reported method[17]. Mice (wild-type: n=10, Sema4D-deficient mice: n=8) were placed in an open field (diameter: 80 cm) in which two identical solid impermeable objects were positioned in the center of respective neighboring quadrants. Mice were allowed to explore the area for three min. One hour later, mice were again placed in the same open field with identical objects, which had been cleaned thoroughly with 50% ethanol, for three minutes. After 24 hours, the mice were again placed in the cleaned field containing one of the original objects and a novel object. Time spent exploring each of the objects was recorded over three minutes. Learning (D score) was calculated as (A-B)/(A+B), where A is the time spent exploring the novel object and B is the time spent exploring the familiar object.

Statistics: Statistical analyses were conducted using StatView (Abacus Concepts, Berkeley, CA, USA). Unless otherwise

specified, data were analyzed by ANOVA and values of $p<0.05$ were regarded as significant. Values are presented as means ± SEM.

Results

Absence of Sema4D protein in the Sema4D-deficient mice brain

As shown in Figure 1a, Western blotting confirmed the absence of Sema4D protein in the Sema4D-deficient mice brain. Since Sema4D and its receptor plexin-B1 are abundant in mouse cerebellum[18-20], we characterized the motor behavioral phenotype of Sema4D-deficient mice using footprint analysis. There were no significant differences between the two genotypes in stride length, base width or front footprint/hind footprint overlap (Figure 1b, stride length; $F(1, 18)=0.031$, $p>0.05$, front limb base width; Student's *t*-test, $p>0.05$, Hind limb base width; Student's *t*-test, $p>0.05$, footprint overlap; Student's *t*-test, $p>0.05$). As seen in Figure 1c, calbindin-immunostaining could not detect any obvious differences in calbindin intensity or the number of Purkinje cells. Furthermore, the dendritic arborization of Purkinje cells appeared normal in Sema4D-deficient mice.

Enhanced locomotor activity in Sema4D-deficient mice

To evaluate the effects of Sema4D gene knockout (KO) on mouse locomotor activity, the horizontal activities of wild-type (WT) and Sema4D-deficient mice in open-field tests were examined. Although the horizontal activities of both types of mice gradually decreased over the four blocks of the test, the extent of activity was significantly higher in Sema4D-deficient mice than in wild-type mice (Figure 2a). The overall difference between the mouse strains and the decrease among time blocks was significant ($F(1,35)=95.669$, $p<0.05$ and $F(3,105)=42.209$, $p<0.05$, respectively). A group difference in block interaction was also significant ($F(3,105)=18.471$, $p<0.05$). A post-hoc test revealed a significant difference between wild-type and Sema4D-deficient mice in each time block. Thus, the open-field tests revealed that Sema4D-deficient mice showed higher locomotor activity than wild-type mice. Sema4D-deficient mice also showed significantly less center time than wild-type controls in the open field (Figure 2b; 4.15 ± 2.89 % versus 9.29

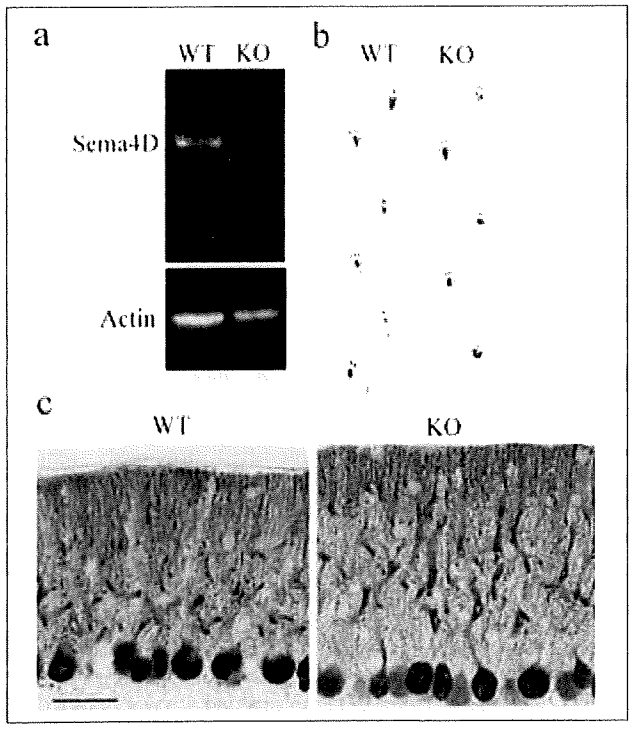

Figure 1: Western blotting analysis demonstrated the absence of Sema4D protein in the Sema4D-deficient mice brain (a). Footprint analysis did not disclose any abnormal gait in Sema4D-deficient mice (b). Calbindin-staining showed no aberrant branching pattern of Purkinje cells in the Sema4D-deficient cerebellum (c). Scale bar, 50 μm. WT=wild type; KO=knockout: Sema4D-deficient mice.

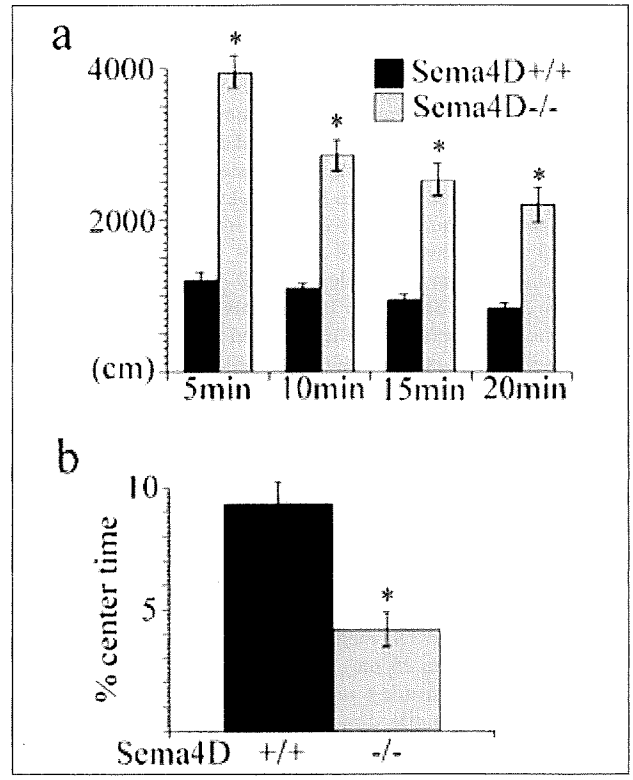

Figure 2: Enhanced locomotor activity of Sema4D-deficient mice in open-field tests. Naive animals were exposed to the open-field test and their locomotor activity (moving distance) was monitored for 20 min (5 min/point). Sema4D-deficient mice showed augmented locomotor activity compared with wild-type mice (a). Sema4D-deficient mice also spent a significantly less percentage of time in the center of the field than wild-type controls (b). +/+: wild-type (n=19); -/-: Sema4D-deficient mice (n=18).

± 4.24%, Student's *t*-test, p<0.05). However, there was no significant difference in the feces number produced during the test between the two genotypes (KO versus WT; 3.28 ± 1.56 versus 2.47 ± 2.41, Student's *t*-test, p>0.05). Furthermore, there was no significant effect of genotype on measures of anxiety-related behavior and general locomotor activity in the elevated plus-maze (%time in closed arm; KO versus WT; 46.63 ± 34.07 % versus 44.97 ± 31.37 %, Student's *t*-test, p>0.05, closed entry; 5.75 ± 4.59 versus 7.56 ± 3.68, Student's *t*-test, p>0.05, open entry; 7.38 ± 3.503 versus 8.33 ± 4.33, Student's *t*-test, p>0.05). There was also no significant effect of genotype on measures of anxiety-related behavior in the light/dark exploration test (% time in dark; KO versus WT; 52.24 ± 27.13 versus 34.21 ± 24.23, Student's t-test, p>0.05, transmission; 11.5 ± 6.89 versus 17.9 ± 8.8, Student's *t*-test, p>0.05). Furthermore, Sema4D-deficient mice showed normal prepulse inhibition to the acoustic startle ($F(1,31)=0.602$, p>0.05, and $F(4,124)=0.673$, p>0.05). Monitoring of locomotor activity for 24 hours in the home cage did not result in any significant differences between the two genotypes ($F(1,16)=0.29$, p>0.05, and $F(16,368)=0.440$, p>0.05).

Superior performance of Sema4D-deficient mice in both adhesive tape removal and rotarod tests

To examine the locomotive power of Sema4D-deficient mice, adhesive tape removal and rotarod tests examining motor function were performed. Sema4D-deficient mice exhibited significantly better performance in the adhesive tape removal test than the wild-type controls (Figure 3a; 1.13 ± 1.71 versus 2.55 ± 1.70, Student's *t*-test, p<0.05). The rotarod test revealed that Sema4D-deficient mice exhibited significantly longer latencies on the rod at an accelerated speed of rotation than wild-type mice (Figure 3b; 257.79 ± 211.04 versus 94.36 ± 75.29, Student's *t*-test, p<0.05). Mean body weight did not differ significantly between wild-type and Sema4D-deficient mice (36.986 ± 1.080 versus 34.779 ± 0.920 g, Student's *t*-test, p>0.05), which excluded the possible influence of body weight on rotarod performance.

Faster swimming speed of Sema4D-deficient mice

To examine whether Sema4D is involved in spatial learning and memory, wild-type and Sema4D-deficient mice were subjected to Morris water maze tests[21]. The ability of both groups to locate the hidden platform improved significantly ($F(27,432)=3.404$, p<0.05) during the training trials, and there was no significant difference between the two groups (Figure 4a, $F(1,16)=2.142$, p>0.05). In the probe test, both wild-type and Sema4D-deficient mice spent more time in the target quadrant than any other quadrant (Figure 4b, $F(3,48)=9.888$, p<0.05), and again there was no significant difference between the two groups (p>0.05, Dunnett's test). Thus, Sema4D-deficient mice showed normal learning and memory for the platform position in the water maze. However, measurement of swimming speed revealed that Sema4D-deficient mice swam significantly faster than wild-type mice (Figure 4c; wild-type mice, 24.9±1.71 cm/s vs. Sema4D-deficient mice, 33.8±2.52 cm/s, p<0.05, Student's *t*-test). The novel object recognition test detected no significant difference in memory between Sema4D-deficient mice and wild-type controls (0.38 ± 0.70 versus 0.40 ± 0.65, Student's *t*-test, p>0.05).

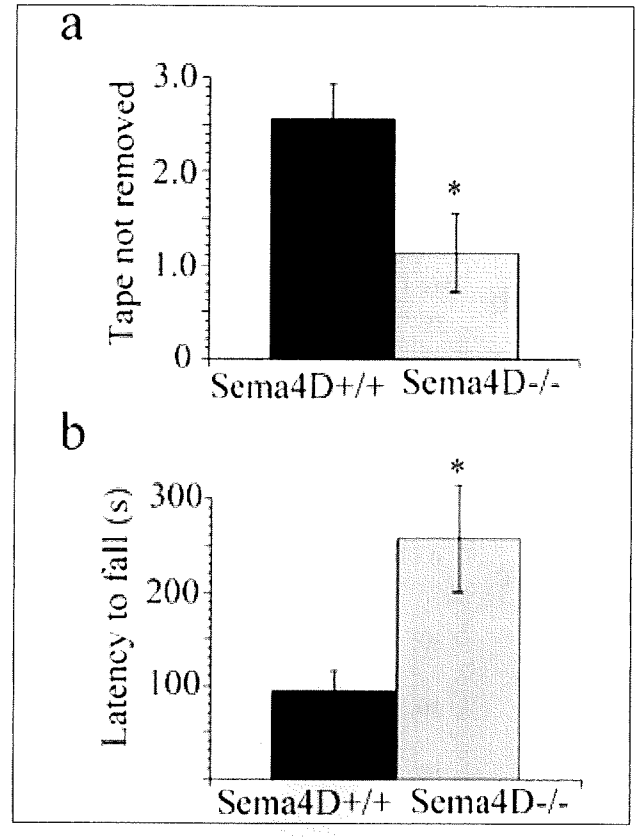

*Figure 3: Superior performance of Sema4D-deficient mice in both adhesive tape removal and rotarod tests. Sema4D-deficient mice exhibited significantly superior performance in the adhesive tape removal test compared with wild-type controls (a). Sema4D-deficient mice acquired significantly longer latencies in an accelerated version of the rotarod test (b). +/+: wild-type; -/-: Sema4D-deficient mice. *p<0.05, Student's t-test.*

Discussion

Our mouse behavioral analyses revealed enhanced motor activity in Sema4D-deficient mice in open field, adhesive tape removal, rotarod and Morris water maze tests. These findings therefore suggest crucial roles of semaphorins in the developmental processes of the internal system regulating mouse motor behavior.

The enhanced activity of Sema4D-deficient mice in the open field, adhesive tape removal and rotarod tests, and swimming in the water maze may be due to abnormal neuronal organization of the basal ganglia or cerebellum generated in the mutant mice. Semaphorins play crucial roles as repulsive or attractive axon guidance molecules during the construction of the neuronal network in central nervous system (CNS) development[5]. Even though calbindin-stained Purkinje cells did not disclose any obvious abnormal phenotype, Sema4D is widely expressed throughout the CNS and Sema4D receptors plexin-B1 and CD72 are localized in mouse cerebellum[18,19,22-25]. Thus, the absence of

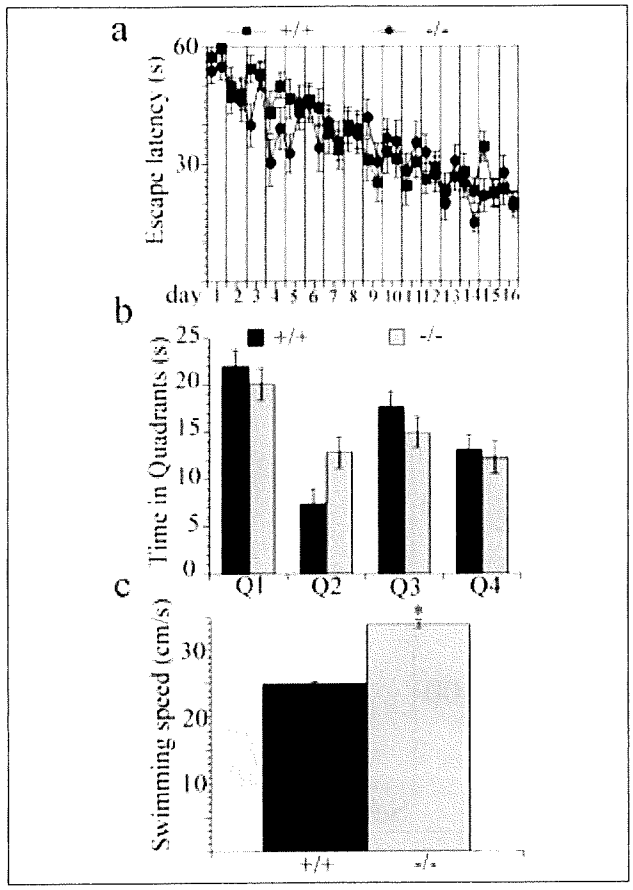

*Figure 4: Faster swimming speed of Sema4D-deficient mice. Sema4D-deficient mice showed normal spatial learning in Morris water maze tasks (a). Sema4D-deficient mice also showed normal spatial memory in the probe test in which the goal in quadrant 1 (Q1) was removed before the test (b). Sema4D-deficient mice exhibited a significantly faster swimming speed than wild-type mice (c). +/+: wild-type; -/-: Sema4D-deficient mice. *p<0.05, Student's t-test.*

Sema4D during brain development may generate abnormal semaphorin signaling induced by compensatory upregulation of several semaphorins in basal ganglia or the cerebellum. As a result, abnormal neural development including increased synaptic growth or axonal overshooting may be generated in regions of the Sema4D-deficient brain, resulting in enhanced motor activity. Future extensive studies are needed to test these possibilities using detailed morphological studies and expression analyses of various semaphorins in the Sema4D-deficient brain. The absence of prepulse inhibition deficits in the acoustic startle reflex suggests that the enhanced motor activity of Sema4D-deficient mice may not be derived from abnormal information processing, as often seen in animal psychiatric disease models[26,27]. It is further suggested that Sema4D-deficient mice may have anxiety-related behavior in the novel open field because of their preference to search around the periphery[28]. However, their anxiety-related behavior was not so strong as to disturb their behavior in the elevated plus maze, light-dark exploration test and water-maze spatial learning. Thus, the anxiety-related behavior seen only in the novel open field may have partly accelerated hyperlocomotion of Sema4D-deficient mice. Sema4D-deficient mice tend to progressively develop autoimmune hepatitis and nephritis with age, and these diseases are mainly mediated by autoantibodies[29]. Antibody-mediated brain injury is known to initially occur in the mouse hippocampus, leading to the development of memory impairment[30]. Since Sema4D-deficient mice preserve normal memory in Morris water maze tasks and the novel recognition memory test, autoantibodies in these animals may not have crossed the blood-brain barrier[31] or generated overt neuropsychiatric syndromes[32-37] or memory impairment[30]. Another possibility may reside in muscular development, since several roles of semaphorins in the muscular system have been reported[38-40]. Since the adhesive tape removal test requires coordinated forelimb use[41-44], subtle altered structures responsible for enhanced motor activity in Sema4D-deficient mice may reside in nigrostriatal regions or cerebellar nuclei rather than the muscular system[45-48]. Thus, the superior performance of Sema4D-deficient mice in the various motor behavior tests may be the first clue toward identifying the developmental step in which semaphorins are crucial for construction of the functional neuronal circuitry governing motor behavior in mice.

In conclusion, our study showed that inhibition of Sema4D activity from an early stage of mouse development results in facilitated motor activity in mouse behavior tests. Provided that regeneration partly recapitulates the developmental process, Sema4D and other semaphorin members may be potential tools in promoting nerve regeneration after CNS injury. It may therefore be possible to develop therapeutic approaches for CNS injury by modulating semaphorin activity[18]. Moreover, our results support the notion that Sema4D provides clues for development of new therapies against CNS injury.

Acknowledgements

The authors thank K. Kubota, M. Kishino, T. Ueyama and E. Yukawa for their encouragement and support. This study was partly supported by Grants-in-Aid for Scientific Research from the Ministry of Education, Science, Sports and Culture, Japan.

References

1. Semaphorin Nomenclature Committee. Unified nomenclature for the semaphorins/collapsins. Cell. 1999;97(5):551-2.
2. Kapfhammer JP. Raper JA. Collapse of growth cone structure on contact with specific neurites in culture. J Neurosci. 1987;7(1): 201-12.
3. Nakamura F. Kalb RG. Strittmatter SM. Molecular basis of semaphorin-mediated axon guidance. J Neurobiol. 2000;44(2): 219-29.
4. Raper JA. Semaphorins and their receptors in vertebrates and invertebrates. Curr Opin Neurobiol. 2000;10(1):88-94.
5. Kruger RP, Aurandt J, Guan KL. Semaphorins command cells to move. Nat Rev Mol Cell Biol. 2005;6(10):789-800.
6. Tamagnone L, Comoglio PM. To move or not to move? Semaphorin signalling in cell migration. EMBO reports. 2004;5(4):356-61.
7. Swiercz JM, Kuner R, Behrens J, Offermanns S. Plexin-B1 directly interacts with PDZ-RhoGEF/LARG to regulate RhoA and growth cone morphology. Neuron. 2002;35(1):51-63.

8. Oinuma I, Ishikawa Y, Katoh H, Negishi M. The semaphorin 4D receptor plexin-B1 is a GTPase activating protein for R-Ras. Science. 2004;305(5685):862-5.
9. Oinuma I, Katoh H, Negishi M. Semaphorin 4D/Plexin-B1-mediated R-Ras GAP activity inhibits cell migration by regulating β1 integrin activity. J Cell Biol. 2006;173(4):601-13.
10. Ito Y, Oinuma I, Katoh H, Kaibuchi K, Negishi M. Sema4D/plexin-B1 activates GSK-3β through R-Ras GAP activity, inducing growth cone collapse. EMBO reports. 2006;7(7):704-9.
11. Paradis S, Harrar DB, Lin Y, Koon AC, Hauser JL, Griffith EC, et al. An RNAi-based approach identifies molecules required for glutamatergic and GABAergic synapse development. Neuron. 2007;53(2):217-32.
12. Shi W, Kumanogoh A, Watanabe C, Uchida J, Wang X, Yasui T, et al. The class IV semaphorin CD100 plays nonredundant roles in the immune system: defective B and T cells activation in CD100-deficient mice. Immunity. 2000;13(5):633-42.
13. Glynn D, Drew CJ, Reim K, Brose N, Morton AJ. Profound ataxia in complexin 1 knockout mice masks a complex phenotype that includes exploratory and habituation deficits. Hum Mol Gent. 2005;14(16):2369-85.
14. Boyce-Rustay JM, Holmes A. Genetic inactivation of the NMDA receptor NR2A subunit has anxiolytic- and antidepressant-like effects in mice. Neuropsychopharmacology. 2006;31(11): 2405-14.
15. Paylor R, Nguyen M, Crawley JN, Patrick J, Beaudet A, Orr-Urtreger A. α7 nicotinic receptor subunits are not necessary for hippocampal-dependent learning or sensorimotor gating: a behavioral characterization of Acra7-deficient mice. Learn Mem. 1998;5(4-5):302-16.
16. Chen L, Cagniard B, Mathews T, Jones S, Koh HC, Ding Y, et al. Age-dependent motor deficits and dopaminergic dysfunction in DJ-1 null mice. J Biol Chem. 2005;280(22):21418-26.
17. Gard PR, Daw P, Mashhour ZS, Tran P. Interactions of angiotensin IV and oxytocin on behaviour in mice. J Renin Angiotensin Aldosterone Syst. 2007;8(3):133-8.
18. Moreau-Fauvarque C, Kumanogoh A, Camand E, Jaillard C, Barbin G, Boquet I, et al. The transmembrane semaphorin Sema4D/CD100, an inhibitor of axonal growth, is expressed on oligodendrocytes and upregulated after CNS lesion. J Neurosci. 2003;23(27):9229-39.
19. Worzfeld T, Püschel AW, Offermanns S, Kuner R. Plexin-B family members demonstrate non-redundant expression patterns in the developing mouse nervous system: an anatomical basis for morphogenetic effects of Sema4D during development. Euro J Neurosci. 2004;19(40):2622-32.
20. Fazzari P, Penachioni J, Gianola S, Rossi F, Eickholt BJ, Maina F, et al. Plexin-B1 plays a redundant role during mouse development and in tumour angiogenesis. BMC Dev Biol. 2007;7:55.
21. Morris RG. Place navigation impaired in rats with hippocampal lesions. Nature. 1982;297(5868):681-3.
22. Tamagnone L, Comoglio PM. Signaling by semaphorin receptors: cell guidance and beyond. Trends Cell Biol. 2000;10(9):377-83.
23. Barberis D, Artigiani S, Casazza A, Corso S, Giordano S, Love CA, et al. Plexin signaling hampers integrin-based adhesion, leading to Rho-kinase independent cell rounding, and inhibiting lamellipodia extension and cell motility. FASEB J. 2004;18(3): 592-4.
24. Kumanogoh A, Kikutani H. The CD100-CD72 interaction: a novel mechanism of immune regulation. Trends Immunol. 2001;22 (12):670-6.
25. Furuyama T, Inagaki S, Kosugi A, Noda S, Saitoh S, Ogata M et al. Identification of a novel transmembrane semaphoring expressed on lymphocytes. J Biol Chem. 1996;271(52):33376-81.
26. Miyakawa T, Leiter LM, Gerber DJ, Gainetdinov RR, Sotnikova TD, Zeng H, et al. Conditional calcineurin knockout mice exhibit multiple abnormal behaviors related to schizophrenia. Proc Natl Acad Sci U S A. 2003;100(15):8987-92.
27. Clapcote SJ, Lipina TV, Millar JK, Mackie S, Christie S, Ogawa F, et al. Behavioral phenotypes of Disc1 missense mutations in mice. Neuron. 2007;54(3):387-402.
28. Holmes A, Yang RJ, Lesch KP, Crawley JN, Murphy DL. Mice lacking the serotonin transporter exhibit 5-HT(1A) receptor-mediated abnormalities in tests for anxiety-like behavior. Neuropsychopharmacology. 2003;28(12):2077-88.
29. Kumanogoh A, Shikina T, Watanabe C, Takegahara N, Suzuki K, Yamamoto M, et al. Requirement for CD100-CD72 interactions in fine-tuning of B-cell antigen receptor signaling and homeostatic maintenance of the B-cell compartment. Int Immunol. 2005;17(10):1277-82.
30. Kowal C, DeGiorgio LA, Nakaoka T, Hetherington H, Huerta PT, Diamond B, et al. Cognition and immunity: antibody impairs memory. Immunity. 2004;21(2):179-88.
31. Kowal C, DeGiorgio LA, Lee JY, Edgar MA, Huerta PT, Volpe BT, et al. Human lupus autoantibodies against NMDA receptors mediate cognitive impairment. Proc Natl Acad Sci USA. 2006;103(52):19854-9.
32. Darnell RB, Posner JB. Paraneoplastic syndromes involving the nervous system. N Engl J Med. 2003;349(16):1543-54.
33. Edwards MJ, Trikouli E, Martino D, Bozi M, Dale RC, Church AJ, et al. Anti-basal ganglia antibodies in patients with atypical dystonia and tics: a prospective study. Neurology. 2004;63 (1):156-8.
34. Fatemi SH. Reelin glycoprotein: structure, biology and roles in health and disease. Mol Psychiatry. 2005;10(3):251-7.
35. Kirvan CA, Swedo SE, Heuser JS, Cunningham MW. Mimicry and autoantibody-mediated neuronal cell signaling in Sydenham chorea. Nat Med. 2003;9(7):914-20.
36. Padmos RC, Bekris L, Knijff EM, Tiemeier H, Kupka RW, Cohen D, et al. A high prevalence of organ-specific autoimmunity in patients with bipolar disorder. Biol Psychiatry. 2004;56(7): 476-82.
37. Snider LA, Swedo SE. PANDAS: current status and directions for research. Mol Psychiatry. 2004;9(10):900-7.
38. Ko JA, Kimura Y, Matsuura K, Yamamoto H, Gondo T, Inui M. PDZRN3 (LNX3, SEMCAP3) is required for the differentiation of C2C12 myoblasts into myotubes. J Cell Sci. 2006;119(Pt 24): 5106-13.
39. Wu H, Wang X, Liu S, Wu Y, Zhao T, Chen X, et al. Sema4C participates in myogenic differentiation in vivo and in vitro through the p38 MAPK pathway. Eur J Cell Biol. 2007;86(6): 331-44.
40. Svensson A, Libelius R, Tågerud S. Semaphorin 6C expression in innervated and denervated skeletal muscle. J Mol Histol. 2008; 39(1):5-13.
41. Whishaw IQ, Suchowersky O, Davis L, Sarna J, Metz GA, Pellis SM. Impairment of pronation, supination, and body co-ordination in reach-to-grasp tasks in human Parkinson's disease (PD) reveals homology to deficits in animal models. Behav Brain Res. 2002;133(2):165-76.
42. Montoya CP, Campbell-Hope LJ, Pemberton KD, Dunnett SB. The "staircase test": a measure of independent forelimb reaching and grasping abilities in rats. J Neurosci Methods. 1991;36(2-3): 219-28.
43. Barnéoud P, Parmentier S, Mazadier M, Miquet JM, Boireau A, Dubédat P, et al. Effects of complete and partial lesions of the dopaminergic mesotelencephalic system on skilled forelimb use in the rat. Neuroscience. 1995;67(4):837-48.
44. Chang JW, Wachtel SR, Young D, Kang UJ. Biochemical and anatomical characterization of forepaw adjusting steps in rat models of Parkinson's disease: studies on medial forebrain bundle and striatal lesions. Neuroscience. 1999;88(2):617-28.
45. Graybiel AM, Aosaki T, Flaherty AW, Kimura M. The basal ganglia and adaptive motor control. Science. 1994;265(5180):1826-31.
46. Saint-Cyr JA, Taylor AE, Nicholson K. Behavior and the basal ganglia. Adv Neurol. 1995;65:1-28.
47. Ito M: The cerebellum and neural control. New York: Raven Press: 1984.
48. Thach WT, Goodkin HP, Keating JG. The cerebellum and the adaptive coordination of movement. Annu Rev Neurosci. 1992;15:403-42.

Signal adaptor DAP10 associates with MDL-1 and triggers osteoclastogenesis in cooperation with DAP12

Masanori Inui[a,1], Yuki Kikuchi[a,1], Naoko Aoki[b], Shota Endo[a], Tsutomu Maeda[a], Akiko Sugahara-Tobinai[a], Shion Fujimura[a], Akira Nakamura[a], Atsushi Kumanogoh[c], Marco Colonna[d], and Toshiyuki Takai[a,2]

[a]Department of Experimental Immunology, Institute of Development, Aging and Cancer, Tohoku University, Seiryo 4-1, Sendai 980-8575, Japan; [b]Department of Pathology, Asahikawa Medical College, Higashi 2-1-1, Midorigaoka, Asahikawa 078-8510, Japan; [c]Department of Immunopathology, Research Institute for Microbial Diseases, Osaka University, Suita, Osaka 565-0871, Japan; and [d]Department of Pathology and Immunology, Washington University School of Medicine, 660 South Euclid, St. Louis, MO 63110

Communicated by Jeffrey V. Ravetch, The Rockfeller University, New York, NY, January 22, 2009 (received for review May 14, 2008)

Osteoclasts, cells of myeloid lineage, play a unique role in bone resorption, maintaining skeletal homeostasis in concert with bone-producing osteoblasts. Osteoclast development and maturation (osteoclastogenesis) is driven by receptor activator of NF-κB ligand and macrophage-colony stimulating factor and invariably requires a signal initiated by immunoreceptor tyrosine-based activation motif (ITAM)-harboring Fc receptor common γ chain or DNAX-activating protein (DAP)12 (also referred to as KARAP or TYROBP) that associates with the cognate immunoreceptors. Here, we show that a third adaptor, YINM costimulatory motif-harboring DAP10, triggers osteoclastogenesis and bone remodeling. DAP10-deficient (*DAP10*$^{-/-}$) mice become osteopetrotic with age, concomitant with a reduction in osteoclasts. The DAP10-associating receptor was identified as myeloid DAP12-associating lectin-1 (MDL-1), whose physiologic function has not been found. MDL-1-mediated stimulation of osteoclast precursor cells resulted in augmented osteoclastogenesis in vitro. MDL-1 associates with both DAP12 and DAP10 in osteoclasts and bone marrow-derived macrophages, where DAP10 association depends almost entirely on DAP12, suggesting a formation of MDL-1–DAP12/DAP10 trimolecular complexes harboring ITAM/YINM stimulatory/costimulatory motifs within a complex that could be a novel therapeutic target for skeletal and inflammatory diseases.

immunoreceptor tyrosine-based activation motif-harboring adaptor | osteoclast development | synergistic signal

Homeostasis of bone tissues is maintained by 2 types of cells, osteoblasts and osteoclasts of mesenchymal and myeloid-cell lineages, respectively. Although osteoblasts are bone-generating cells, osteoclasts are present on bone erosive surfaces in the marrow and play a unique role in bone resorption, maintaining the mass and structure of bone tissues in collaboration with osteoblasts. Osteoclast development and maturation (osteoclastogenesis) depends on receptor activator of NF-κB ligand (RANKL) and macrophage-colony stimulating factor (M-CSF) (1, 2). M-CSF interaction with its receptor c-fms, a receptor tyrosine kinase expressed on osteoclasts, supports the survival of osteoclast precursor cells (3, 4). However, binding of RANKL to its receptor RANK on the osteoclast precursor cell surface induces TNF receptor-associated factor 6 (TRAF6) and NF-κB activation, leading to transcription of a master transcription factor for osteoclastogenesis, nuclear factor of activated T cells (NFAT)c1 (5, 6). Full activation and induction of NFATc1 for this intracellular signal initiated by RANKL, however, invariably require the tyrosine phosphorylation-based stimulating signal initiated by the Fc receptor common γ chain (FcRγ) or DNAX-activating protein (DAP)12 (also known as KARAP or TYROBP) (7–14).

FcRγ and DAP12 are immunoreceptor tyrosine-based activation motif (ITAM)-harboring, membrane-bound signal adaptors expressed in leukocytes that associate with and support the cell-surface expression of various activating-type immunoreceptors of the Ig superfamily or C-type lectin family. They primarily mediate a Src-family kinase-initiated activation signal, leading to a series of events including Syk kinase recruitment, triggering of calcium signaling mediated by phospholipase Cγ (PLCγ), and activation of the MAPK cascade, culminating in cell proliferation and cytokine production as the output of cellular responses. In osteoclast precursor cells, FcRγ and DAP12 associate with several cognate cell-surface immunoreceptors (9) such as osteoclast-associated receptor (OSCAR) (15) and paired Ig-like receptor-A (PIR-A) (16, 17) or triggering receptor expressed on myeloid cells-2 (TREM-2) (18) and signal regulatory protein β1 (SIRPβ1) (19), respectively. Mice deficient in both FcRγ and DAP12 exhibit a markedly excessive bone mass (osteopetrosis) caused by a severe defect in the development of osteoclasts (9, 10). In vitro osteoclastogenesis was greatly impaired when bone marrow cells from DAP12-deficient (*DAP12*$^{-/-}$) mice or monocytes from *DAP12*$^{-/-}$ humans were cultured with RANKL and M-CSF (12–14) or such cells from FcRγ/DAP12 double-deficient (*FcRγ*$^{-/-}$*DAP12*$^{-/-}$) mice were cocultured with osteoblasts (9, 10). Moreover, we demonstrated that RANKL stimulation of osteoclast precursor cells led to tyrosine phosphoryation of DAP12 and FcRγ and activation of PLCγ (9). These results indicate the indispensable roles of these ITAM-harboring signal adaptors and associated receptors in osteoclastogenesis. This notion is further supported by the fact that the bone marrow cells in mice lacking Syk or PLCγ also fail to differentiate into mature osteoclasts (10, 20). Btk and Tec kinases were identified very recently as the link between RANK activation and ITAM phosphorylation of FcRγ and DAP12 (21).

Although FcRγ and DAP12 have been identified as indispensable stimulators for osteoclastogenesis (9, 10), a markedly reduced, but small number of osteoclasts was still found in *FcRγ*$^{-/-}$*DAP12*$^{-/-}$ mice (9), suggesting the existence of other activating adaptors or pathways that promote or compensate for osteoclastogenesis in vivo. A candidate molecule that might operate in the absence of FcRγ and DAP12 could be DAP10, which is also a membrane-associated signal adaptor harboring a costimulatory YINM motif and is cognate to DAP12 in the immune system (22, 23), but it remains unknown whether DAP10 is involved in the skeletal system. DAP10 is expressed broadly on hematopoietic cells, such as monocytes and macrophages (22, 23), NK cells, and CD8$^+$ T cells (23), and functions through its association with NKG2D, the only known DAP10 partner receptor that recognizes

Author contributions: A.N., A.K., and T.T. designed research; M.I., Y.K., S.E., A.S.-T., and S.F. performed research; N.A., T.M., and M.C. contributed new reagents/analytic tools; M.I., Y.K., S.E., A.S.-T., and S.F. analyzed data; and M.I., Y.K., and T.T. wrote the paper.

The authors declare no conflict of interest.

[1]M.I. and Y.K. contributed equally to this work.

[2]To whom correspondence should be addressed. E-mail: tostakai@idac.tohoku.ac.jp.

This article contains supporting information online at www.pnas.org/cgi/content/full/0900463106/DCSupplemental.

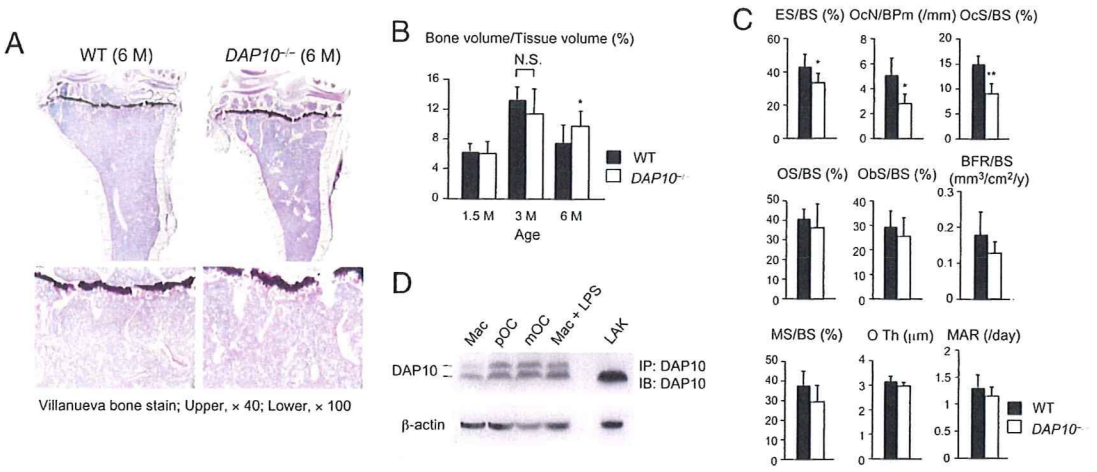

Fig. 1. Bone histological analysis reveals osteopetrosis in *DAP10*$^{-/-}$ mice developing with age. (*A*) Villanueva bone staining of tibial sections from female 6-month-old WT and *DAP10*$^{-/-}$ mice. Trabecular bones were increased, particularly in the metaphysis of *DAP10*$^{-/-}$ mice. (*B*) Bone morphometric analysis reveals the bone volume was increased in *DAP10*$^{-/-}$ mice at 6 months of age but not at 1.5 and 3 months of age, indicating osteopetrosis developing with age in the mice. Data are expressed as means ± SD ($n = 9$, female). *, $P < 0.05$. N.S., not significant. (*C*) Analysis of bone morphometric parameters in 6-month-old WT and *DAP10*$^{-/-}$ mice reveals reduced osteoclast parameters in *DAP10*$^{-/-}$ animals but comparable osteoblast parameters. BS, bone surface; ES, erosive surface; OcN, osteoclast number; BPm, bone perimeter; OcS, osteoclast surface; OS, osteoid surface; ObS, osteoblast surface; BFR, bone formation rate; MS, mineral surface; O Th, osteoid thickness; MAR, mineral apposition rate. Data are expressed as means ± SD ($n = 9$, female). *, $P < 0.05$; **, $P < 0.01$. (*D*) DAP10 protein expression was examined by immunoprecipitation and immunoblot analysis of cell extracts prepared from bone marrow-derived macrophages (Mac), pOCs, mOCs, macrophages stimulated with 0.1 μg/ml LPS for 24 h, and splenic DX5$^+$ NK cells stimulated with 1,000 units/mL of IL-2 for 4 days. As a loading control, a β-actin blot is shown.

stress-induced MHC class I-like ligands (22, 24). DAP10 is unique in that it does not have an ITAM in its cytoplasmic domain but instead contains a different tyrosine-based motif, YINM, that is similar to those found in costimulatory receptors such as CD28 and ICOS and binds to the p85 subunit of PI3K (22) and Grb2 (23), leading to the triggering of calcium signaling and cytotoxicity in NK cells.

We attempted to clarify whether DAP10 could be a hidden signal adaptor molecule that promotes osteoclastogenesis. Here, we demonstrate the physiological function of myeloid DAP12-associating lectin-1 (MDL-1) (25) and the significance of its novel amplifying role in osteoclastogenesis through the cooperation of DAP10 with DAP12.

Results

DAP10-Deficient Mice Exhibit Mild Osteopetrosis Caused by a Reduction in the Osteoclast Number in Bone Tissues. To clarify whether DAP10 could be an activating adaptor for osteoclast development, we first performed bone morphometric analyses of DAP10-deficient (*DAP10*$^{-/-}$) mice (see *SI Text*). Tibial bone sections from 6-month-old *DAP10*$^{-/-}$ mice were found to exhibit slight increases in the metaphyses and trabecular bones, indicating mild osteopetrosis (Fig. 1*A*). Osteopetrosis was not evident in mice at 1.5 and 3 months of age, but it was significant in 6-month-old *DAP10*$^{-/-}$ mice (Fig. 1*B*). This observation was in sharp contrast to that for *DAP12*$^{-/-}$ mice, in which mild osteopetrosis was evident even in 1.5-month-old animals and was significant afterward at least up to 12 months of age (12). This difference is probably because the contribution of DAP10 to osteoclast development depends on DAP12 (see below). A small number of tartrate-resistant acid phosphatase (TRAP)$^+$ osteoclasts was seen in bone tissues from FcRγ/DAP12/DAP10 triple knockout (*FcRγ*$^{-/-}$*DAP12*$^{-/-}$*DAP10*$^{-/-}$) mice and *FcRγ*$^{-/-}$*DAP12*$^{-/-}$ mice (Fig. S1), supporting the above notion.

Bone morphometric analyses of the tibia of these mice at 6 months of age revealed significant reductions in osteoclast-related parameters (Fig. 1*C Top*), indicating reductions in the number and function of osteoclasts in *DAP10*$^{-/-}$ mice, while keeping comparable values for osteoblastic parameters (Fig. 1*C Middle* and *Bottom*). These parameters for 1.5- and 3- month-old *DAP10*$^{-/-}$ mice were comparable with those for WT mice (Fig. S2). These results indicate that the increased bone mass in *DAP10*$^{-/-}$ mice was caused by attenuated osteoclastogenesis, although the overall magnitude of the defect was apparently smaller than that in *DAP12*$^{-/-}$ mice, as judged from the occurrence of osteopetrosis in *DAP12*$^{-/-}$ animals at as early as 1.5 months of age (12). We found that DAP10 protein is expressed in immature, prefusion osteoclasts (pOCs), mature, multinucleated osteoclasts (mOCs), and bone marrow-derived macrophages in vitro (Fig. 1*D Upper*), but not in osteoblasts (Fig. S3) on immunoblot analysis with DAP10-specific antibodies (Fig. S4), suggesting a role of DAP10 in the development of osteoclasts.

In Vitro Osteoclastogenesis Was Impaired in the Absence of DAP10. With the RANKL/M-CSF system, culturing of bone marrow-derived monocyte/macrophage lineage cells (BMMs) as osteoclast precursor cells from *DAP10*$^{-/-}$ mice resulted in a significant reduction in the number of TRAP$^+$ mOCs, especially with suboptimal concentrations of RANKL and M-CSF (5–20 and 1–10 ng/mL, respectively) (Fig. 2*A* and *B*). Concomitant with the reduction in mOCs, the resorptive pit area formed by *DAP10*$^{-/-}$ mOCs was also reduced (Fig. 2*C*). In the presence of suboptimal concentrations of RANKL, an excess concentration (100 ng/mL) of M-CSF did not rescue the reduced osteoclastogenesis (Fig. 2*D*). Reduced osteoclastogenesis was also observed with the osteoblast coculture system (Fig. 2*E*). Flow cytometric analyses (Fig. S5) verified that the cell-surface expression levels of the M-CSF receptor c-fms and the RANKL receptor RANK on pOCs were comparable among B6, *DAP10*$^{-/-}$, *DAP12*$^{-/-}$, and *DAP12*$^{-/-}$*DAP10*$^{-/-}$ (Fig. S6) cells, indicating that the reduced development of *DAP10*$^{-/-}$ osteoclasts is not caused by reduced expression levels of c-fms and RANK but a deficit in DAP10. These observations suggest that the RANKL/M-CSF-mediated signal is insufficient in *DAP10*$^{-/-}$ osteoclast precursor cells.

Identification of MDL-1 as a Distinct Cell-Surface Receptor That Associates with DAP10 in Osteoclasts. How does DAP10 participate in osteoclastogenesis? Although DAP10 physiologically associates with the only known partner, NKG2D, in immune cells (22), we failed to detect a significant amount of NKG2D mRNA in osteoclast lineage cells after GeneChip (9) and RT-PCR analyses (Fig. S7).

IMMUNOLOGY

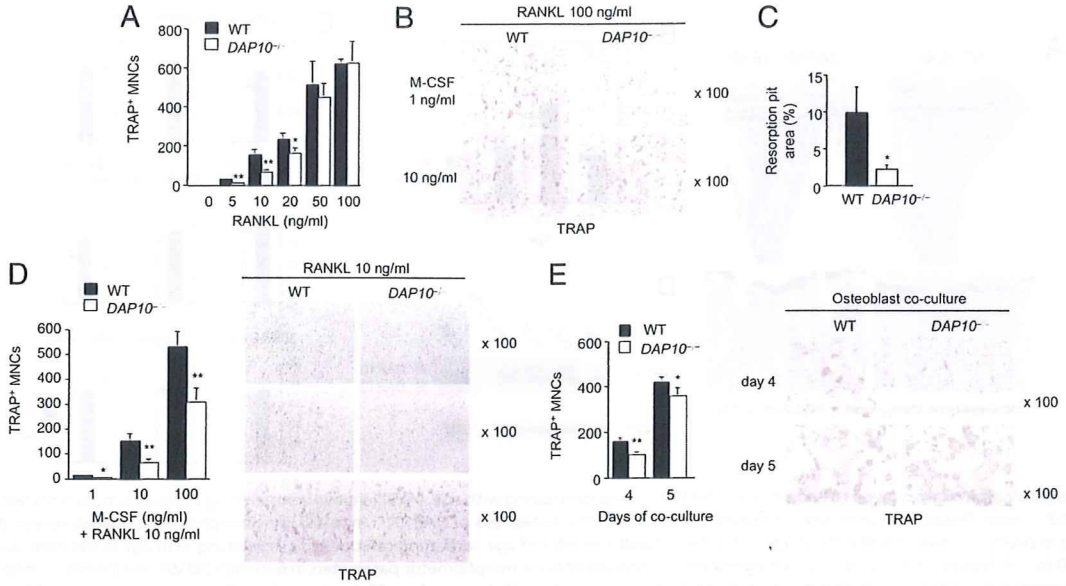

Fig. 2. Osteoclast development and function are impaired in an in vitro culture. (*A*) Reduced osteoclastogenesis in *DAP10*$^{-/-}$ bone marrow-derived monocyte/macrophage lineage cells (BMMs) stimulated with suboptimal concentrations of RANKL in the presence of 20 ng/mL M-CSF. TRAP^{+} multinucleated cells (MNCs) were counted. (*B*) Reduced osteoclastogenesis in *DAP10*$^{-/-}$ BMMs with suboptimal concentrations of M-CSF (1 or 10 ng/mL) in the presence of sufficient RANKL (100 ng/mL). (*C*) Reduced pit formation of *DAP10*$^{-/-}$ osteoclasts obtained in culture in the presence of 100 ng/mL RANKL and 20 ng/mL M-CSF. (*D*) Reduced osteoclastogenesis in *DAP10*$^{-/-}$ BMMs stimulated with 10 ng/mL RANKL and 1, 10, or 100 ng/mL M-CSF. (*E*) Reduced osteoclastogenesis in *DAP10*$^{-/-}$ BMMs cocultured with osteoblasts. Data are representative of 3 separate experiments with similar results and are expressed as means ± SD for triplicate cultures. *, $P < 0.05$; **, $P < 0.01$.

Therefore, the formation of a functional NKG2D–DAP10 complex in osteoclasts is unlikely. To find a candidate receptor that associates with DAP10, we prepared macrophages, pOCs, and mOCs from B6 and *DAP10*$^{-/-}$ mice, which were surface-biotinylated, either glycosidase-treated or left untreated, and then immunoprecipitated with anti-DAP10 antibodies. Comparison of the profiles for surface-biotinylated proteins of DAP10-sufficient and -deficient cells enabled us to detect a discrete band of ≈27-kDa glycosylated protein species, whose deglycosylated form was ≈18 kDa (Fig. S8*A*). We excised a gel strip containing this protein and subjected it to TOF/MS analysis (see *SI Text*). Sixty-six tryptic peptide sequences obtained were searched for in the NCBInr database (www.protein.sdu.dk/gpmaw/GPMAW/Databases/NCBInr/ncbinr.html), and 6 murine proteins were shown to be significant hits, among which C-type lectin domain family 5 member A (i.e., MDL-1) (25) was the only notable one in the context of our investigation (Fig. S8*B*). The expression of mRNA for MDL-1 was confirmed by RT-PCR analysis of samples from pOCs, mOCs, and macrophages as described (26) (Fig. S8*C*). MDL-1 was identified originally (25) as a type II transmembrane glycoprotein of the C-type lectin superfamily (Fig. S8*D*), expressed as a DAP12-dependent manner as both long and short forms possibly arising from alternative splicing, but neither the physiological role of nor the ligand for MDL-1 has been elucidated. Based on the knowledge obtained in these preceding studies, our present observations indicate that MDL-1 could associate with DAP10 in addition to DAP12 in macrophages and osteoclasts and might function as an activating receptor in osteoclasts. Although C-type lectin superfamily molecules are often expressed on the cell surface as a disulfide-linked homodimer like NKG2D or Ly49C (22, 27), or a heterodimer such as CD94–NKG2A (28), the results from our immunoblot analyses indicated that the majority of the MDL-1 short and long forms exist as monomers (*SI Text* and Fig. S8*E*).

DAP10 Forms an MDL-1–DAP12/DAP10 Trimolecular Complex Depending Almost Solely on DAP12. To determine whether MDL-1 expression solely depends on DAP12 or not, we performed flow cytometry of MDL-1 expression on macrophages and pOCs from mice deficient in either DAP12, DAP10, DAP12 and DAP10, or FcRγ (Fig. 3*A*). The MDL-1 expression levels on macrophages and pOCs were not changed by FcRγ deletion, but were reduced markedly in the absence of DAP10 and decreased to a minimum with either DAP12 or DAP12 and DAP10 double deletion. We verified that the MDL-1 mRNA levels in pOCs from these mutant mice were not reduced when compared with that in pOCs from B6 mice (Fig. S9). Thus, MDL-1 cell-surface expression primarily depends on DAP12, and partially, but substantially also depends on DAP10.

Given that the DAP12-associated receptor TREM-2 (18) has been implicated in osteoclastogenesis (29–31), it would be interesting to determine whether the expression of TREM-2 is also diminished in *DAP10*$^{-/-}$ and *DAP12*$^{-/-}$*DAP10*$^{-/-}$ osteoclasts like that of MDL-1. Our flow cytometric analysis (Fig. 3*B*) revealed that TREM-2 expression on pOCs did not change with the deficiency of DAP10 or DAP10 and DAP12, and in the deficiency of DAP12, as reported (29), indicating that the TREM-2 expression itself does not depend on DAP10 or DAP12, which is in sharp contrast to the case of MDL-1. However, this observation does not exclude the possibility that DAP10 could enhance TREM-2–DAP12-mediated signaling.

To confirm the DAP12- and DAP10-dependent expression of MDL-1, lysates of macrophages, pOCs, and mOCs derived from B6, *DAP10*$^{-/-}$, and *DAP12*$^{-/-}$ mice were immunoprecipitated with anti-MDL-1 polyclonal antibodies and then subjected to immunoblotting with antibodies to MDL-1 or DAP10 and DAP12. As shown in Fig. 4*A*, top 2 panels), immunoprecipitation/immunoblotting analyses with MDL-1 antibodies and with or without *N*-glycosidase treatment revealed that macrophages, pOCs and mOCs from B6 mice (lanes 1–3) and macrophage-like RAW cells (lane 11) exhibited high expression of a diffuse, glycosylated 38- to 45-kDa protein species corresponding to the highly glycosylated, monomeric long form of MDL-1, and several discrete and a diffuse protein species ≈20–28 kDa corresponding to the differently glycosylated, monomeric short form of MDL-1. These protein species were confirmed to migrate at the positions consistent with the predicted core sizes for MDL-1 long and short forms after

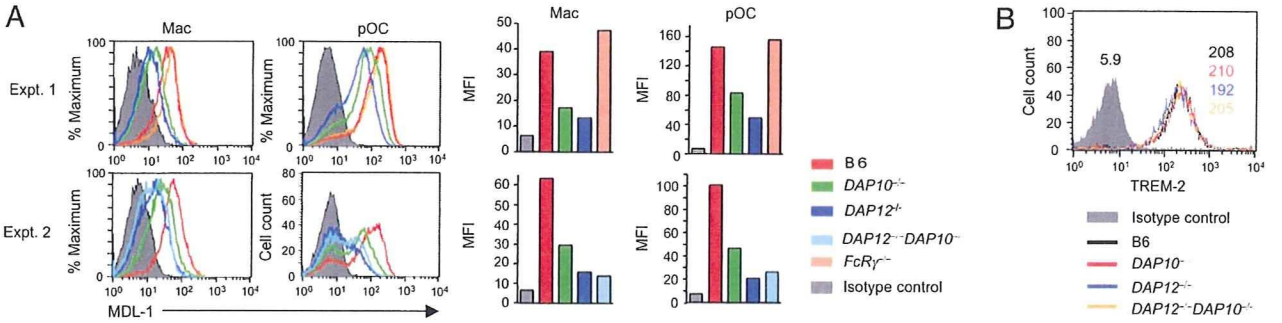

Fig. 3. Cell surface expression of MDL-1 depends on DAP12 and is enhanced by DAP10. (*A*) The results or flow cytometric analysis of surface MDL-1 expression in bone marrow-derived macrophages (Mac) and pOCs are shown as histograms and as graphs for mean fluorescence intensity (MFI) of each histogram profile. Macrophages and pOCs obtained from B6 (red), *DAP10*$^{-/-}$ (green), *DAP12*$^{-/-}$ (blue), and *FcRγ*$^{-/-}$ (orange) (experiment 1) or *DAP12*$^{-/-}$*DAP10*$^{-/-}$ (light blue) (experiment 2) mice were stained with phycoerythrin-conjugated anti-MDL-1 mAb or an isotype control, and then subjected to flow cytometry. (*B*) Flow cytometric analysis of TREM-2 expression on pOCs obtained from B6 (black), *DAP10*$^{-/-}$ (red), *DAP12*$^{-/-}$ (blue), and *DAP12*$^{-/-}$*DAP10*$^{-/-}$ (orange) mice. MFI value of each histogram is shown.

treatment with the combination of *N*- and *O*-glycosidases and neuraminidase (Fig. S10; see also Fig. S8*E*). We observed less abundant, long and short form MDL-1 bands for samples of macrophages, pOCs and mOCs from *DAP10*$^{-/-}$ and *DAP12*$^{-/-}$ mice (Fig. 4*A*, lanes 4–9).

As shown in Fig. 4*A* (bottom 2 panels), we observed DAP12 and DAP10 coimmunoprecipitation with MDL-1 for all 3 cell populations from WT B6 mice (lanes 1–3) and in RAW cells (lane 11). For *DAP10*$^{-/-}$ cells, we observed DAP12 coprecipitation with MDL-1 (lanes 4–6) as expected from the results of flow cytometric analysis. Rather curiously, however, we did not detect DAP10–MDL-1 coprecipitation for *DAP12*$^{-/-}$ cells (lanes 7–9). To check the overall expression levels of DAP10 and DAP12, and their possible interaction, we performed immunoprecipitation and immunoblot analyses of these 2 adaptors in macrophage lysates from B6, *DAP10*$^{-/-}$ and *DAP12*$^{-/-}$ mice (Fig. 4*B*). It was evident that both DAP10 and DAP12 were expressed in total macrophage lysates (Fig. 4*B Upper*, lanes 7 and 8 and Fig. 4*B Lower*, lanes 1 and 2). Interestingly, DAP10 expression was markedly reduced in the absence of DAP12 (Fig. 4*B Upper*, *lane 9* and Fig. 4*B Lower*, lane 3) but importantly not lost completely (Fig. 4*B Upper*, lane 6), suggesting that the DAP10 protein is unstable in the absence of DAP12. This finding is in sharp contrast to in the case of IL-2-activated killer cells (LAK) in which DAP10 is abundantly expressed in the absence of DAP12 (Fig. 4*B Upper*, lane 10 and Fig. 4*B Lower*, lane 5) and is functional because DAP10-dependent NKG2D expression is normal in the absence of DAP12 (Fig. S11). Also, it was verified that DAP10 was coimmunoprecipitated with DAP12 (Fig. 4*B Upper*, lanes 2 and 4), suggesting that DAP10 is a component of one or more DAP12-receptor complexes in macrophages and RAW cells. To examine directly the association among MDL-1, DAP10, and DAP12, we performed immunoprecipitation/immunoblot analysis of RAW cell extracts with polyclonal antibodies specific to each molecule (Fig. 4*C*). We found that DAP10 and DAP12 immunoprecipitation resulted in coprecipitation of DAP12 and DAP10, respectively, in addition to MDL-1. To examine the presence of DAP12–DAP10 heterodimers associating with MDL-1, total lysates of pOCs were immunoprecipitated with anti-MDL-1 mAb, separated by SDS/PAGE under nonreducing conditions, and then immunoblotted with anti-DAP12 or DAP10 antibodies (Fig. 4*D*). We found the 16-kDa protein species in B6 pOCs that was reactive with both DAP12 and DAP10 antibodies (Fig. 4*D*, lanes 1 and 3) and was lost in the DAP10 deficiency (Fig. 4*D*, lane 2), suggestive of the DAP12–DAP10 heterodimer. Collectively, these results suggest that the DAP12–MDL-1 complex is a prototype structure for the surface expression of MDL-1, and that DAP10 association with MDL-1 almost solely depends on the presence of DAP12–MDL-1, forming an MDL-1–DAP12/DAP10 trimolecular complex.

MDL-1 Functions as a Positive Regulator of Osteoclastogenesis. To determine how MDL-1 functions in osteoclastogenesis, we stimulated BMMs from B6 mice with a plate-bound anti-MDL-1 mAb and found an increase in RANKL-induced mOCs (Fig. 5*A*). To further confirm the activating function of MDL-1, we examined the effect of suppression of mRNA for MDL-1 by the RNA silencing technique. Transfection of MDL-1 siRNA, but not nontargeting siRNA, reduced the level of MDL-1 mRNA (Fig. S12) and led to the reduced number of mOCs (Fig. 5*B*). These results led to our conclusion that MDL-1 functions as a positive regulator of osteoclastogenesis.

Discussion

Murine NKG2D can be expressed as a NKG2D–DAP12 complex or as a NKG2D–DAP10 complex, both of which are capable of initiating a signal (32, 33). In addition, recent stoichiometric analysis revealed that the human NKG2D homodimer can associate with 2 homodimeric forms of DAP10, resulting in the formation of a hexameric structure (34). Thus, binding of a single ligand can result in the phosphorylation of 4 DAP10 chains, which may be relevant as to the sensitivity of the receptor, in particular in the situation of low ligand density (34). It has been pointed out that a hexameric NKG2D complex is assembled in activated murine NK cells, which incorporates 1 DAP10 and 1 DAP12 homodimer. The formation of such a trimolecular hexamer could be functionally relevant, because the 2 homodimers initiate distinct signaling cascades: DAP12 activates the Syk/ZAP70 pathway, and DAP10 signals through the PI3K pathway (24, 35, 36). SIRPβ1 (19) is also capable of associating with either the DAP12 or DAP10 homodimer or the DAP12/DAP10 heterodimer in the RBL-2H3 leukemic mast cell line (37).

In sharp contrast to NKG2D, MDL-1 expression solely depends on the association with DAP12 and is accelerated by the additional association with DAP10, possibly through, most simply, the ultimate formation of an MDL-1–DAP12/DAP10 trimolecular complex, although we do not exclude a possibility of any unidentified molecule intervening MDL-1–DAP12 and DAP10, or a possible sharing of DAP10 between MDL-1–DAP12 and any unidentified receptor–DAP10: the unidentified molecule or receptor could also be an MDL-1 itself. In any case, MDL-1 cannot be expressed robustly on the cell surface as an MDL-1–DAP10 complex. It has not ever been clarified whether MDL-1 itself is expressed as a monomeric form or a homodimer, or both (25, 38). Our immunoblot analysis (Fig. 4*A* and Fig. S8*E*) indicates that the majority of MDL-1 is expressed as a monomeric form on macrophages, pOCs, and mOCs, while it also did not exclude the possibility of the presence of minor populations containing homodimeric or long form–short form heterodimeric complexes or heterooligomeric complexes with other membrane proteins such as CD94 (28). In an MDL-1–DAP12/DAP10 trimeric complex, monomeric MDL-1

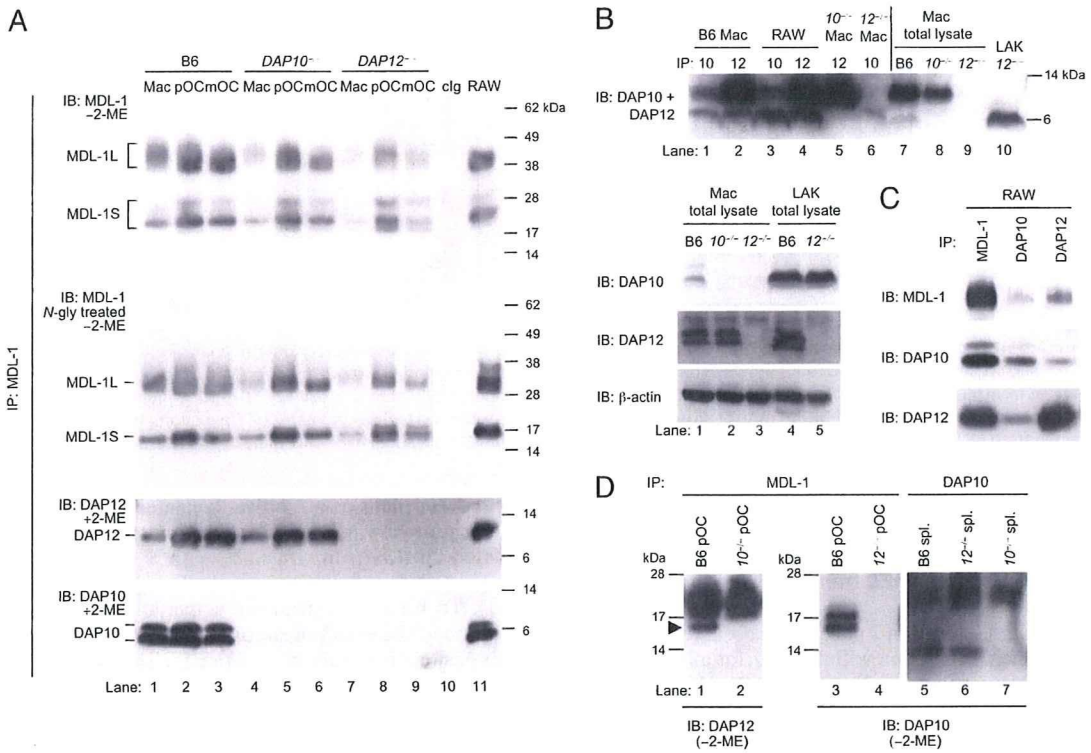

Fig. 4. DAP10 forms an MDL-1–DAP12/DAP10 trimolecular complex depending almost solely on DAP12. (*A*) Immunoprecipitation and immunoblot analysis of MDL-1 (top 2 panels) and its DAP10/DAP12 association (bottom 2 panels). Cell lysates of bone marrow-derived macrophages (Mac), pOCs, and mOCs from B6, *DAP10*$^{-/-}$ and *DAP12*$^{-/-}$ mice were immunoprecipitated with anti-MDL-1 antibodies, treated with *N*-glycosidase or left untreated, separated by SDS/PAGE under nonreducing (−2-ME) or reducing conditions (+2-ME), and immunoblotted with anti-MDL-1, anti-DAP12, or anti-DAP10 antibodies. Lysates of RAW264.7 cells immunoprecipitated with anti-MDL-1 or control Ig (clg) were used as positive and negative controls, respectively. Long-form and short-form MDL-1 are denoted. (*B*) Immunoprecipitation and immunoblot analysis of DAP10 and DAP12 in macrophages. Cell lysates of macrophages (Mac) cultured from bone marrow cells of B6, *DAP10*$^{-/-}$ and *DAP12*$^{-/-}$ mice, and of RAW, as a positive control, were immunoprecipitated with anti-DAP10 or DAP12 antibodies, and immunoblotted with anti-DAP10 and anti-DAP12 antibodies (*Upper*, lanes 1–6). Total lysates of macrophages from B6, *DAP10*$^{-/-}$, and *DAP12*$^{-/-}$ mice, and of IL-2-activated splenic NK cells (LAK) from *DAP12*$^{-/-}$ mice are simultaneously blotted (*Upper*, lanes 7–10). Note that DAP10 band becomes weak in the absence of DAP12 for macrophages (*Upper*, lane 9) but not for LAK (*Upper*, lane 10) and that DAP12 immunoprecipitation yields DAP10 coprecipitation (*Upper*, lanes 2 and 4). The disappearance of the DAP10 band in the absence of DAP12 for macrophages but not for LAK is reproduced (*Lower*, lanes 3 and 5). (*C*) DAP10 coprecipitates with DAP12 and vice versa together with MDL-1. Lysates of RAW cells were immunoprecipitated with either anti-MDL-1, anti-DAP10, or anti-DAP12 anbitodies, separated by SDS/PAGE under reducing conditions, and then immunoblotted with each antibody. (*D*) DAP10 possibly forms an MDL-1–DAP12–DAP10 triplex. Total cell lysates of pOCs and splenocytes (spl.) from B6, *DAP10*$^{-/-}$, and *DAP12*$^{-/-}$ mice were immunoprecipitated with anti-MDL-1 mAb or anti-DAP10 antibodies, separated by SDS/PAGE under nonreducing conditions, and immunoblotted with anti-DAP12 or DAP10 antibodies. The robust and seemingly triplet bands migrating at 18–25 kDa detected with anti-DAP12 antibodies in B6 pOCs (lane 1) are assigned to DAP12–DAP12 homodimers with different glycosylation, because these protein species do not react with anti-DAP10 antibodies (lane 3) and are present even in the absence of DAP10 (lane 2). Immunoprecipitation of splenocyte samples with anti-DAP10 antibodies followed by detection with anti-DAP10 revealed a ≈13-kDa band for the less-glycosylated or nonglycosylated DAP10–DAP10 homodimer that presumably associates with NKG2D on NK cells in splenocytes (lanes 5 and 6; see also Figs. S4, S6, and S11). This form of homodimeric DAP10–DAP10 was not detected in B6 pOC samples (lane 3). The less-glycosylated or nonglycosylated monomeric 6-kDa DAP10 is truly a component of the MDL-1 complex (see *A*, lane 2), suggesting the pairing with a different molecule. The 16-kDa band (lane 1, arrowhead), detected with anti-DAP12 antibodies in B6 pOCs, is attributable to a heterodimer of DAP12 paired with less-glycosylated or nonglycosylated DAP10, because it was lost in the DAP10 deficiency (lane 2). Consistent with this notion, the 16-kDa band was detectable also with anti-DAP10 antibodies in B6 pOCs (lane 3). The 18-kDa band, reactive with anti-DAP10 antibodies (lane 3), is probably also a DAP12–DAP10 heterodimer in a different glycosylation state, whose supposed disappearance in DAP10 deletion might be masked by the DAP12 homodimer bands (lane 2).

would associate with a disulfide-bonded DAP12–DAP10 heterodimer, thereby allowing the full cascade of events including Syk and PLCγ1 activation via ITAM-harboring DAP12 (9, 10), and PI3K and Grb2–Vav1 recruitment via YINM-harboring DAP10 located just proximal to DAP12. By being positioned very close to each other in a trimeric complex, the 2 adaptor molecules could collaborate intimately, enabling them to signal much more efficiently than as singlets.

We showed (9) that TREM-2 (18) and SIRPβ1 could accelerate osteoclastogenesis via the DAP12 signal. Then, is it pertinent to suppose that MDL-1–DAP12/DAP10 is as equally important as TREM-2–DAP12 and SIRPβ1–DAP12? In a normal situation, a restricted number of DAP12 molecules might be competitively recruited by at least 3 different receptors, MDL-1, TREM-2, and SIRPβ1, which evokes a presence of any complex mechanism for functional allotment among them. If, for example, DAP12 can preferentially associate with TREM-2 than others, it indirectly reduces the chance of MDL-1 associating with DAP12, and thus lowers the expression level of MDL-1–DAP12/DAP10. We speculate that TREM-2– and SIRPβ1–DAP12 have to cooperate with MDL-1–DAP12/DAP10 for full-blown osteoclastogenesis. Relative significance of the individual receptors in osteoclastogenesis awaits experimental verifications such as examinations in MDL-1-deficient mice.

A defect in the DAP12–TREM-2 function leads to the development of heritable Nasu–Hakola disease in humans (11, 14). Involvement of MDL-1–DAP12/DAP10 in osteoclastogenesis suggests that Nasu–Hakola disease by DAP12 deficiency may also

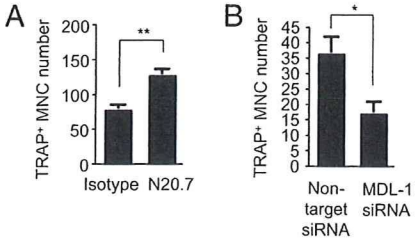

Fig. 5. MDL-1 functions as a positive regulator of osteoclastogenesis. (*A*) Stimulation of pOCs with plate-bound MDL-1 mAb leads to enhanced osteoclastogenesis. Bone marrow-derived monocyte/macrophage lineage cells (BMMs) prepared from B6 mice were stimulated with plate-bound N20.7 mAb or an isotype control antibody in the presence of RANKL/M-CSF. The number of $TRAP^+$ cells (>3 nuclei) was determined. (*B*) Reduced osteoclastogenesis by MDL-1 siRNA. BMMs transfected with MDL-1 or nontargeting siRNA were cultured for 4 days in the presence of M-CSF, and then further cultured with RANKL for 4 days. The number of $TRAP^-$ cells (>3 nuclei) was determined. Data are expressed as means ± SD of triplicate culture. *, $P < 0.05$; **, $P < 0.01$.

include a defect in the MDL-1 function, albeit it has not been tested yet. The *MDL-1* gene is located on human chromosome 7q33 and murine chromosome 6B2 as a single copy gene (official symbol, *Clec5a*), where no disease relation has been mapped to date. MDL-1 is a member of a large complex of genes termed the C-type lectin domain (CLEC) family (39), although both the murine and human MDL-1 genes are apart from the CLEC locus present in murine 6F3 and human chromosome 12. The CLEC family comprises 13 structurally-related molecules such as Dectin-1 and Dcir encoded by genes at the 6F3 region, which is adjacent to the locus for the NKG2 family and the Ly49 family. A recent gene targeting study has revealed the significance of Dcir in autoimmune diseases (40). Our present study suggests that an altered function of MDL-1 could also be related to osteopetrosis, osteoporosis, rheumatoid arthritis, and other inflammatory diseases, where osteoclast/macrophage development and function is perturbed or dysregulated.

During preparation of our article, we found out that DAP10 has been coimmunoprecipitated with Ly49H and Ly49D from IL-2-cultured mouse NK cells (41), and that DAP10 and DAP12 supports Ly49H surface expression on NK cells, and the Ly49H–DAP10 receptor complex is functional (M. Orr and L. L. Lanier, personal communication). Therefore, DAP10 could be a more versatile adaptor in terms of the receptor expression/function than we previously thought. Our current identification of MDL-1 as the newly recognized receptor that associates with DAP10 may open up an additional avenue for dissecting the full spectrum of DAP10- and DAP12-mediated activation cascade of various cells not only in terms of osteoclastogenesis but also in other cellular development and function and diseases. After submission of this article, it was reported that MDL-1 can bind the dengue virion and initiate proinflammatory cytokine release (42). It is of no doubt that identification of physiological MDL-1 ligands will facilitate our understanding of the roles of MDL-1–DAP12/DAP10 in health and disease.

Materials and Methods

All statistics were generated with Student's *t* test. $P < 0.05$ was considered significant. Other methods are detailed in *SI Text* and refs. 9 and 33).

ACKNOWLEDGMENTS. We thank Nobuo Kanazawa for critical comments, Nicholas Halewood for editorial assistance, and Yumi Ito for outstanding technical support. This work was supported in part by the Core Research for Evolutional Science and Technology Program of the Japan Science and Technology Agency, a Grant-in-Aid from the Ministry of Education, Culture, Sports, Science, and Technology of Japan, a grant from the 21st Century Center of Excellence Program for Innovative Therapeutic Development Toward the Conquest of Signal Transduction Diseases, and the Global Center of Excellence Program for Conquest of Signal Transduction Diseases with Network Medicine.

1. Karsenty G, Wagner EF (2002) Reaching a genetic and molecular understanding of skeletal development. *Dev Cell* 2:389–406.
2. Rodan GA, Martin TJ (2000) Therapeutic approaches to bone diseases. *Science* 289:1508–1514.
3. Teitelbaum SL, Ross FP (2003) Genetic regulation of osteoclast development and function. *Nat Rev Genet* 4:638–649.
4. Boyle WJ, Simonet WS, Lacey DL (2003) Osteoclast differentiation and activation. *Nature* 423:337–342.
5. Takayanagi H, et al. (2002) Induction and activation of the transcription factor NFATc1 (NFAT2) integrate RANKL signaling in terminal differentiation of osteoclasts. *Dev Cell* 3:889–901.
6. Takayanagi H (2007) The role of NFAT in osteoclast formation. *Ann N Y Acad Sci* 1116:227–237.
7. Lanier LL, Corliss BC, Wu J, Leong C, Phillips JH (1998) Immunoreceptor DAP12 bearing a tyrosine-based activation motif is involved in activating NK cells. *Nature* 391:703–707.
8. Tomasello E, et al. (1998) Gene structure, expression pattern, and biological activity of mouse killer cell activating receptor-associated protein (KARAP)/DAP-12. *J Biol Chem* 273:34115–34119.
9. Koga T, et al. (2004) Costimulatory signals mediated by the ITAM motif cooperate with RANKL for bone homeostasis. *Nature* 428:758–763.
10. Mócsai A, et al. (2004) The immunomodulatory adapter proteins DAP12 and Fc receptor γ-chain (FcRγ) regulate development of functional osteoclasts through the Syk tyrosine kinase. *Proc Natl Acad Sci USA* 101:6158–6163.
11. Paloneva J, et al. (2000) Loss-of-function mutations in TYROBP (DAP12) result in a presenile dementia with bone cysts. *Nat Genet* 25:357–361.
12. Kaifu T, et al. (2003) Osteopetrosis and thalamic hypomyelinosis with synaptic degeneration in DAP12-deficient mice. *J Clin Invest* 111:323–332.
13. Nataf S, et al. (2005) Brain and bone damage in KARAP/DAP12 loss-of-function mice correlate with alterations in microglia and osteoclast lineages. *Am J Pathol* 166:275–286.
14. Paloneva J, et al. (2003) DAP12/TREM2 deficiency results in impaired osteoclast differentiation and osteoporotic features. *J Exp Med* 198:669–675.
15. Kim N, Takami M, Rho J, Josien R, Choi Y (2002) A novel member of the leukocyte receptor complex regulates osteoclast differentiation. *J Exp Med* 195:201–209.
16. Kubagawa H, Burrows PD, Cooper MD (1997) A novel pair of immunoglobulin-like receptors expressed by B cells and myeloid cells. *Proc Natl Acad Sci USA* 94:5261–5266.
17. Yamashita Y, et al. (1998) Genomic structures and chromosomal location of p91, a novel murine regulatory receptor family. *J Biochem* 123:358–368.
18. Bouchon A, Dietrich J, Colonna M (2000) Cutting edge: Inflammatory responses can be triggered by TREM-1, a novel receptor expressed on neutrophils and monocytes. *J Immunol* 164:4991–4995.
19. Dietrich J, Cella M, Seiffert M, Bühring HJ, Colonna M (2000) Cutting edge: Signal-regulatory protein β1 is a DAP12-associated activating receptor expressed in myeloid cells. *J Immunol* 164:9–12.
20. Mao D, Epple H, Uthgenannt B, Novack DV, Faccio R (2006) PLCγ2 regulates osteoclastogenesis via its interaction with ITAM proteins and GAB2. *J Clin Invest* 116:2869–2879.
21. Shinohara M, et al. (2008) Tyrosine kinases Btk and Tec regulate osteoclast differentiation by linking RANK and ITAM signals. *Cell* 132:794–806.
22. Wu J, et al. (1999) An activating immunoreceptor complex formed by NKG2D and DAP10. *Science* 285:730–732.
23. Chang C, et al. (1999) Cutting edge: KAP10, a novel transmembrane adapter protein genetically linked to DAP12 but with unique signaling properties. *J Immunol* 163:4651–4654.
24. Raulet DH (2003) Roles of the NKG2D immunoreceptor and its ligands. *Nat Rev Immunol* 3:781–790.
25. Bakker AB, Baker E, Sutherland GR, Phillips JH, Lanier LL (1999) Myeloid DAP12-associating lectin (MDL)-1 is a cell surface receptor involved in the activation of myeloid cells. *Proc Natl Acad Sci USA* 96:9792–9796.
26. Humphrey MB, et al. (2004) The signaling adapter protein DAP12 regulates multinucleation during osteoclast development. *J Bone Miner Res* 19:224–234.
27. Dam J, et al. (2003) Variable MHC class I engagement by Ly49 natural killer cell receptors demonstrated by the crystal structure of Ly49C bound to H-$2K^b$. *Nat Immunol* 4:1213–1222.
28. Phillips JH, et al. (1996) CD94 and a novel associated protein (94AP) form a NK cell receptor involved in the recognition of HLA-A, HLA-B, and HLA-C allotypes. *Immunity* 5:163–172.
29. Humphrey MB, et al. (2006) TREM2, a DAP12-associated receptor, regulates osteoclast differentiation and function. *J Bone Miner Res* 21:237–245.
30. Cella M, et al. (2003) Impaired differentiation of osteoclasts in TREM-2-deficient individuals. *J Exp Med* 198:645–651.
31. Colonna M, Turnbull I, Klesney-Tait J (2007) The enigmatic function of TREM-2 in osteoclastogenesis. *Adv Exp Med Biol* 602:97–105.
32. Rabinovich B, et al. (2006) NKG2D splice variants: A reexamination of adaptor molecule associations. *Immunogenetics* 58:81–88.
33. Gilfillan S, Ho EL, Cella M, Yokoyama WM, Colonna M (2002) NKG2D recruits two distinct adapters to trigger NK cell activation and costimulation. *Nat Immunol* 3:1150–1155.
34. Garrity D, Call ME, Feng J, Wucherpfennig KW (2005) The activating NKG2D receptor assembles in the membrane with two signaling dimers into a hexameric structure. *Proc Natl Acad Sci USA* 102:7641–7646.
35. Lanier LL (2005) NK cell recognition. *Annu Rev Immunol* 23:225–274.
36. Wu J, Cherwinski H, Spies T, Phillips JH, Lanier LL (2000) DAP10 and DAP12 form distinct, but functionally cooperative, receptor complexes in natural killer cells. *J Exp Med* 192:1059–1068.
37. Anfossi N, et al. (2003) Contrasting roles of DAP10 and KARAP/DAP12 signaling adaptors in activation of the RBL-2H3 leukemic mast cell line. *Eur J* Immunol 33:3514–3522.
38. Takaki R, Watson SR, Lanier LL (2006) DAP12: An adapter protein with dual functionality. *Immunol Rev* 214:118–129.
39. Kanazawa N (2007) Dendritic cell immunoreceptors: C-type lectin receptors for pattern recognition and signaling on antigen-presenting cells. *J Dermatol Sci* 45:77–86.
40. Fujikado N, et al. (2008) Dcir deficiency causes development of autoimmune diseases in mice due to excess expansion of dendritic cells. *Nat Med* 14:176–180.
41. Coudert JD, Scarpellino L, Gros F, Vivier E, Held W (2008) Sustained NKG2D engagement induces cross-tolerance of multiple distinct NK cell activation pathways. *Blood* 111:3571–3578.
42. Chen ST, et al. (2008) CLEC5A is critical for dengue-virus-induced lethal disease. *Nature* 453:672–676.

J Clin Immunol (2009) 29:1–11
DOI 10.1007/s10875-008-9263-7

Immune Semaphorins: Novel Features of Neural Guidance Molecules

Masayuki Mizui · Atsushi Kumanogoh · Hitoshi Kikutani

Received: 10 November 2008 / Accepted: 10 November 2008 / Published online: 6 December 2008

Abstract
Introduction The immune and nervous system have various common features in the functional characteristics. Both have an intricate network of synaptic connections and an exquisite communication system that enables intercellular signal transduction. They also share a number of messenger molecules such as cytokines and chemical mediators.
Discussion Semaphorins, well-defined axonal guidance molecules in the nervous system, also play critical roles in immune regulation. Various types of semaphorins, including secreted, transmembrane, truncated, and glycosylphosphatidylinositol-anchored forms, function during immune responses. However, some semaphorins utilize receptors in the immune system that are distinct from receptors in the nervous system.
Conclusion This review presents a current overview of 'immune semaphorins' and their receptors, providing insight into the pleiotropic activity of this protein family.

Keywords Semaphorins · semaphorin receptors · immune regulation · autoimmune disease · allergy

M. Mizui · H. Kikutani (✉)
Department of Molecular Immunology,
Research Institute for Microbial Diseases, Osaka University,
3-1 Yamada-oka,
Suita, Osaka, Japan
e-mail: kikutani@ragtime.biken.osaka-u.ac.jp

A. Kumanogoh
Department of Immunopathology,
Research Institute for Microbial Diseases, Osaka University,
3-1 Yamada-oka,
Suita, Osaka, Japan

M. Mizui · A. Kumanogoh · H. Kikutani
WPI Immunology Frontier Research Center, Osaka University,
3-1 Yamada-oka,
Suita, Osaka, Japan

Introduction

The immune response is composed of a series of cell–cell contacts, including the interaction between T cells and antigen-presenting cells (APCs) such as B cells, macrophages, and dendritic cells (DCs). Such cell–cell contact elicits the activation response, which determines clonal expansion and effector function of T cells. The area of cell contact is called an 'immunological synapse', which is structurally similar to the synapse that connects pairs of neurons. There are many similarities between the immune and nervous systems: Both are highly networked systems and share chemical mediators (e.g., prostaglandins) and cytokines (e.g., interleukin 1β (IL-1β), IL-2, tumor necrosis factor alpha (TNFα)) [1].

Semaphorins, true to their name, are axonal guidance factors that function during neural development. Semaphorins were initially identified as chemorepulsive molecules among the neural attractive and repulsive cues in the extracellular environment that guide axon pathfinding [2]. More than 20 types of semaphorins have been identified to date [3]. Semaphorins are currently known to have diverse actions: They can exert repulsive, attractive, or bifunctional effects depending on the biological context in which they are encountered [4]. They are secreted or membrane-associated glycoproteins that have been grouped into eight classes. The semaphorin family carries a long stretch of conserved 'sema domain' in the N terminus. The semaphorins range in size from 400 to 1,000 amino acids depending on additional C-terminal sequence motifs such as immunoglobulin domain, thrombospondin domain, or glycosylphosphatidylinositol (GPI) linkage site. Class I and II semaphorins are found in invertebrates, whereas class III to VII semaphorins are found in vertebrates and class VIII are viral. In vertebrates, proteins in semaphorin classes IV

to VII are membrane-associated, whereas those in class III are secreted. The major semaphorin receptors are plexin family proteins [5, 6]. Plexins are categorized into four groups and also carry sema domains. The plexin intracellular domain shares homology with the GTPase-activating protein domain, indicating that semaphorin-plexin signaling is involved in cellular morphology [7]. Another group of semaphorin receptors, neuropilins (Nrp-1 and Nrp-2), form receptor complexes with plexin-A family members and exclusively binds to class III semaphorins [8].

Semaphorins also play important roles in other biological processes, including cardiac morphogenesis [9], vascular [10, 11] and epithelial growth and invasion [12, 13], tumor progression [14], and immune regulation [15–17]. Interestingly, in organs other than the brain, semaphorin receptor plexins associate with several effector molecules. For example, Off-track (Otk) or vascular endothelial growth factor receptor 2 (VEGFR2) associate with plexin-A1 during cardiac development [18]and Met associates with plexin-B1 in epithelial cells [13]. Notably, in the immune system, some semaphorins use non-plexin receptors, such as CD72 [19] and TIM-2 [20] (see below and Fig. 1). These observations provide insight into the diversity of semaphorin function. In this review, we will present the latest knowledge of semaphorins and their receptors, which are involved in the immune responses.

Sema4D

Sema4D-CD72 Interaction in the Immune System

Sema4D, also known as CD100, is the first semaphorin family member protein identified in the immune system [21, 22]. Sema4D is a 150-kDa cell surface transmembrane protein that forms a homodimer. In the immune system, Sema4D is expressed abundantly in resting T cells but only weakly in resting B cells and APCs [23, 24], and its

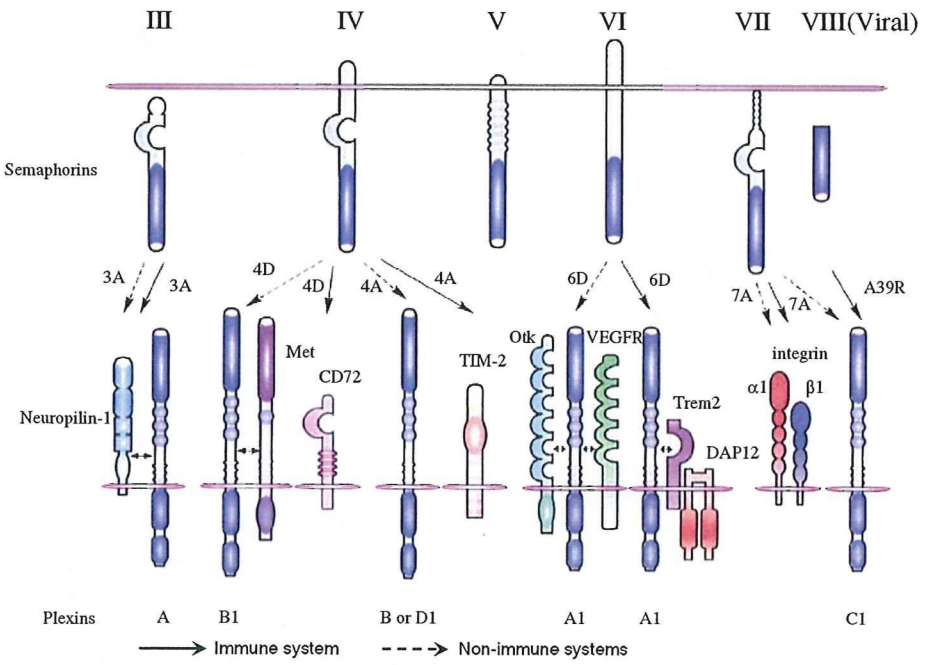

Fig. 1 Representative semaphorins and their multiple receptors. Among the eight classes of semaphorins, class I and II semaphorins are found in invertebrates (not shown in figure) and class III–VII are vertebrate semaphorins. Classes II and III and viral semaphorins are secreted, whereas class IV–VI are transmembrane. Class VII represents GPI-anchored proteins. Sema3A directly binds to Nrp-1, which results in transduction of plexin-A-mediated signals. Although Sema4D binds to plexin-B1 in brain and transduces chemorepulsive signals, plexin-B1 couples with Met in epithelial cells and induces Sema4D-mediated cell outgrowth. In the immune system, Sema4A binds to CD72, which enhances B cell and DC activation. Sema4A recognizes plexin-B and D1 in the non-immune systems but uses TIM-2 as a receptor for T cell activation in the immune system. During cardiogenesis, plexin-A1 associates with Off-track (*Otk*) or VEGFR2 at distinct sites and transduces Sema6D signals. However, plexin-A1 forms a receptor complex with TREM-2-DAP12 in the immune system, which is critical for DC activation and osteoclastogenesis. Sema7A has two types of receptors: $\alpha 1\beta 1$ integrin for macrophage activation and plexin-C1 for inhibition of cell adhesion. Viral semaphorin A39R also recognizes plexin-C1 and modulates dendritic cell function

expression is upregulated upon cellular activation [19]. Cumulative evidence indicates that Sema4D can function as a ligand. Sema4D-transfected B cells promote their aggregation and survival in vitro. In addition, recombinant soluble Sema4D or Sema4D-expressing cells enhance in vivo antibody production as well as in vitro B-cell responses [21, 25].

Two types of proteins, plexin-B1 and CD72, have been identified as Sema4D receptors. The major receptor for Sema4D in the nervous system is plexin-B1. Sema4D binding to plexin-B1 downregulates guanosine triphosphatase (GTPase) activity of R-Ras, a member of the Ras superfamily of small GTP-binding proteins, and induces growth cone collapse in hippocampal neuron [26]. Moreover, plexin-B1 forms a functional receptor complex with Met in epithelial cells and Sema4D binding to plexin-B1 promotes epithelial invasive growth [13]. However, in the immune system, CD72 is the predominant receptor for Sema4D [19]. CD72, a 45-kDa C-type lectin family protein, is constitutively expressed on B cells and APCs. CD72 contains two immunoreceptor tyrosine-based inhibitory motifs in the cytoplasmic domain that recruit the tyrosine phosphatase SHP-1 upon B-cell receptor (BCR) stimulation [27, 28]. SHP-1 associates with many inhibitory receptors, including CD22 and killer cell immunoglobulin-like receptors to inhibit the functions of B cells and natural killer (NK) cells, respectively. B cells from CD72-deficient mice undergo hyper-proliferation and have a rapid calcium response following BCR stimulation compared to B cells from wild-type mice [29]. Therefore, CD72 functions as a negative regulator of B cells.

The molecular mechanisms governing Sema4A-CD72-mediated regulation of BCR signals have been uncovered. Treatment of B cells with soluble Sema4D inhibits phosphorylation of CD72 and its association with SHP-1 [19]. Conversely, CD72 and SHP-1 are constitutively associated in B cells from Sema4D-deficient mice. Stimulation-induced association of CD72 with the BCR complex is inhibited by Sema4D. Finally, Sema4D-deficient B cells are hypo-responsive to BCR stimulation compared to wild-type B cells [25]. Collectively, these results indicate that Sema4D enhances B cell activation by 'turning off' inhibitory CD72 signals [30] (Fig. 2a).

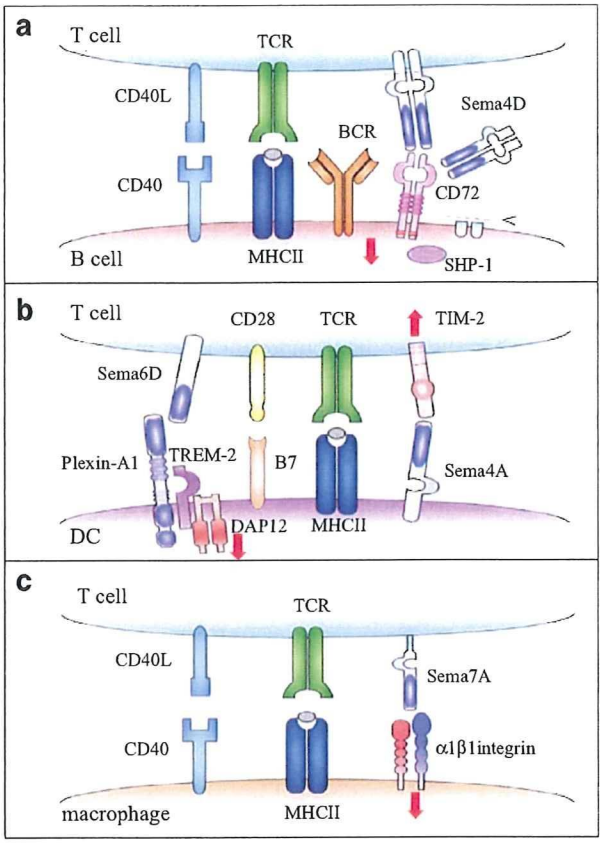

Fig. 2 Semaphorins in immune cell interactions. Semaphorins act at various phase and stage of immune cell interactions. **a** During T-cell-mediated B-cell activation, engagement of CD72 by Sema4D induces dephosphorylation of CD72 and dissociation from SHP-1, which results in enhancement of BCR signals. Sema4D can also be cleaved proteolytically and function as a soluble form in an autocrine/paracrine manner. **b** During T cell–DC interaction, Sema6D on T cells can activate DCs through the plexin-A1-TREM-2-DAP12 receptor complex. Sema4A on DCs binds to TIM-2 and activates T cells. **c** T-cell-mediated inflammatory responses require antigen–MHC class II–TCR interaction and CD40L–CD40 signals. However, the interaction between Sema7A and α1β1 integrin is also critical for activation of inflammatory cells such as macrophages

Sema4D and Immune Homeostasis

Changes in the BCR activation threshold due to alteration of signaling molecules downstream of BCR are thought to affect B-cell survival and turnover [31]. Sema4D is also involved in the homeostatic maintenance of B-cell subsets. In young Sema4D-deficient mice, the population of $CD5^+$ B1 cells is significantly reduced, although other B-cell subsets seem normal [25]. However, the proportion of $CD21^{hi}CD23^{lo}$ marginal zone B (MZB) cells in Sema4D-deficient mice gradually increases with advancing age [32]. Expansion of MZB cells is involved in defective BCR signaling, whereas increased B1 cell numbers are observed in mice lacking inhibitory receptors such as CD22 [33] and CD72 [29], suggesting that the requirement for BCR signaling differs among B-cell subsets. Therefore, a higher BCR signaling threshold may promote the development or survival of MZB cells but may be detrimental for the development of B1 cells in Sema4D-deficient mice.

Marginal zone, the region at the interface between lymphoid white pulp and non-lymphoid red pulp in the spleen, has been proposed as a site for sequestration of

autoreactive cells [34]. MZB cells may play a role in homeostasis and tolerance and in host defense and may be important for the induction of autoimmune diseases. Notably, the expansion of MZB cells in aged Sema4D-deficient mice is accompanied by the production of a variety of autoantibodies, including anti-ssDNA, anti-dsDNA, rheumatoid factors, anti-Sjogren's syndrome A, and anti-ribonucleoprotein [32]. Furthermore, these mutant mice exhibit marked perivascular leukocyte infiltration in several tissues, including salivary gland, liver, and kidney, and thickened basement membrane along with the deposition of immunoglobulin G in the kidney glomeruli. Although a limited number of aged CD72-deficient mice exhibit substantial amounts of autoantibodies [35], mice lacking both Sema4D and CD72 show no evidence of autoimmune disease [32]. These observations suggest that breakdown of Sema4D-CD72-mediated B-cell homeostasis may promote the expansion of MZB cells and the development of autoimmune diseases.

Sema4D and T-Cell-Mediated Immunity

As described above, T cells are the major Sema4D-producing cells in the immune system. However, Sema4D-deficient T cells respond normally to in vitro stimulation. Moreover, soluble Sema4D does not affect T-cell activation, suggesting that Sema4D has no direct effect on T cells. In contrast, soluble Sema4D enhances the surface expression of CD80, CD86, and major histocompatibility complex (MHC) class II on DCs [36]. The function of Sema4D in T cell–DC interactions has been addressed in vitro. Sema4D-sufficient $CD4^+$ T cells can differentiate normally into cytokine-secreting effector cells even when cultured with antigen and Sema4D-deficient DCs. In contrast, Sema4D-deficient $CD4^+$ T cells fail to differenciate even in the presence of Sema4D-sufficient DCs. Therefore, Sema4D expressed on T cells acts on DCs to promote their activation and maturation possibly through interaction with CD72, which in turn enhances T-cell activation [37].

The importance of Sema4D in T-cell-mediated immunity has also been verified using the mutant mice. After immunization of Sema4D-deficient mice with protein antigens, proliferative responses of $CD4^+$ T cells from draining lymph nodes are significantly impaired, as is cytokine production after antigen restimulation. Moreover, Sema4D-deficient mice are resistant to experimental autoimmune encephalomyelitis (EAE) induced by myelin oligodendrocyte glycoprotein (MOG)-derived peptide, a mouse disease model for multiple sclerosis (MS) because generation of MOG-specific T cells is impaired in these mice [36]. Sema4D-deficient mice are also protected from experimental immune complex glomerulonephritis due to reduced T-cell activation and humoral immune responses [38]. These observations indicate that Sema4D is crucially involved in the activation and differentiation of T cells.

Functional Soluble Sema4D Extracellular Domain Fragment

Upon activation, Sema4D is proteolytically cleaved and released from the cell surface, suggestive of an autocrine and/or paracrine mechanism of action [39]. Soluble form of Sema4D released from T and B cells retains biological activity, and a variety of functions has been documented. In vivo antibody responses against T-cell-dependent antigens and generation of antigen-specific T cells are enhanced in transgenic mice expressing a truncated form of Sema4D [40]. It is also noteworthy that a significant amount of soluble Sema4D is detectable in the sera of wild-type mice immunized with a T-cell-dependent antigen and in the sera of an autoimmune-prone MRL/lpr mice, a model of systemic lupus erythematosus [39]. Here, the levels of soluble Sema4D correlate well with titers of antigen-specific antibody or autoantibodies, although soluble Sema4D is undetectable in the sera of non-immunized or normal mice. Interestingly, soluble Sema4D from T cells can also affect neuron and glial cells. In neuroinflammatory diseases such as MS and virus-induced demyelination, inappropriate cross-talk between activated T cells infiltrating the central nervous system (CNS) can sustain the onset and progression of demyelination and axonal degradation. Soluble Sema4D released from activated T cells collapses oligodendrocyte process extensions and triggers neural cell apoptosis. Indeed, high levels of soluble Sema4D in the cerebrospinal fluid are detected in patients suffering with human T lymphotropic virus type 1-induced neuroinflammatory demyelination (TSP/HAM) [41]. These findings suggest that soluble Sema4D is involved in various phases of pathological responses.

Sema4A

Sema4A-Mediated Regulation of T Helper Cell Differentiation

Like Sema4D, Sema4A is also a member of the class IV transmembrane semaphorin subfamily. Sema4A is expressed in a broad range of adult tissues, including brain, lung, spleen, kidney, and testis [20]. The Sema4A expression profile in immune cells is unique. Sema4A is constitutively expressed in all mouse DC subset but is barely detectable in resting or naive T cells. T cell receptor (TCR) stimulation induces transient Sema4A expression within 24 h, but its expression rapidly decreases thereafter.

However, when T cells are cultured under T helper type 1 (Th1)-polarizing conditions, high Sema4A expression is sustained throughout the culture period, whereas Sema4A expression is diminished in Th2-polarizing conditions [42]. Analysis of Sema4A-deficient mice has revealed that DC-derived Sema4A and Th1 cell-derived Sema4A play distinct functional roles in the development of T-cell-mediated immunity, as described below.

When T cells are cultured in Th1-polarizing conditions, Sema4A-deficient naive $CD4^+$ T cells fail to differentiate into interferon gamma (IFN-γ)-producing cells. In contrast, Sema4A-deficient naive cells normally differentiate into IL-4-producing cells under Th2 conditions. This selective defect in Th1 differentiation of Sema4A-deficient T cells is associated with reduced expression of IL-12 receptor β chain and T-bet, a transcription factor essential for Th1 development. Interestingly, normal Th1 differentiation of Sema4A-deficient T cells is fully restored by either the addition of soluble Sema4A protein or coculture with wild-type T cells. Thus, Sema4A on T cells may promote Th1 differentiation through cognate interaction between T cells. Sema4A-mediated regulation of Th cell differentiation has also been confirmed in vivo. The generation of IFN-γ-producing antigen-specific T cells is impaired in Sema4A-deficient mice immunized with Th1-inducing agents such as heat-killed *Propionibacterium acnes*. Conversely, Sema4A-deficient mice mount enhanced Th2 responses when infected with *Nippostrongylus brasiliensis*, a Th2-inducing intestinal nematode [42]. Moreover, it is striking that Sema4A-deficient mice of a Th2-prone BALB/c strain spontaneously develop atopic dermatitis (unpublished data).

Sema4A in DCs

The presence of recombinant soluble Sema4A protein substantially enhances the proliferation and IL-2 production of naive T cells from wild-type mice after TCR stimulation, which suggests that Sema4A contributes to T-cell activation through T cell–DC interactions. Indeed, Sema4A-deficient DCs poorly stimulate allogeneic T cells, despite the fact that Sema4A-deficient DCs mature normally and produce cytokines in response to lipopolysaccharide or anti-CD40. Generation of antigen-specific T cells after immunization with various antigens is consistently defective in Sema4A-deficient mice [42]. These observations indicate that Sema4A expressed on DCs is involved in the initial activation of T cells. Furthermore, when Sema4A-deficient DCs are transferred into Sema4A-sufficient mice, proliferation and IL-2 secretion of antigen-specific T cells are impaired, but substantial numbers of IFN-γ-producing T cells are generated. In contrast, when Sema4A-sufficient DCs are transferred into Sema4A-deficient mice, proliferation and IL-2 secretion are substantial but IFN-γ-production is defective in antigen-specific T cells. Collectively, DC-derived Sema4A is involved in T cell priming, and T cell-derived Sema4A is required for Th1 differentiation.

TIM-2 as a Sema4A Receptor

Thus far, Sema4A receptor in the nervous system has not been identified. However, Sema4A-deficient mice show severe retinal degeneration, suggesting that Sema4A interacts with a specific receptor(s) in the CNS [43]. On the other hand, in the cardiovascular system, plexin-D1 has been identified as a Sema4A receptor and Sema4A–plexin-D1 interaction suppresses angiogenesis [11]. This interaction modulates VEGF-mediated endothelial cell migration and proliferation intracellularly, by suppressing VEGF–VEGFR2-induced activation of Rac1, Akt, and integrins. In the immune system, T cell immunoglobulin and mucin domain-2 (TIM-2), a type I transmembrane protein, has been identified as a Sema4A-binding partner [20]. The TIM gene family consists of eight members (TIMs 1–8, but 5–8 are predictive) in mouse and three members (TIMs 1, 3, and 4) in human. The chromosomal region containing the TIM family is thought to be associated with allergic diseases because the IL-4 cytokine gene cluster, IL-12p40, gene and IL-12 regulator gene are also included in this region. The TIM locus has been positionally cloned by screening congenic mice for the susceptibility in an asthma disease model [44]. Indeed, genetic polymorphisms in both TIM-1 and TIM-3 correlate with susceptibility to asthma in human. There is also much evidence that TIM family proteins are expressed by immune cells and involved in several phases of immune responses [45–47]. Although the TIM-2 gene is not detected in humans, mouse TIM-2 shares great identity with mouse TIM-1 and is thought to be an orthologue of human TIM-1 [48].

Sema4A binding induces tyrosine phosphorylation of the cytoplasmic tail of TIM-2; therefore, TIM-2 seems to transduce Sema4A signals (Fig. 2b) [20]. TIM-2 is expressed on activated $CD4^+$ T cells and is preferentially upregulated during Th2 differentiation. A study using recombinant soluble TIM-2 suggests that TIM-2 plays a role in the regulation of Th2 responses [49]. Administration of soluble TIM-2 during the initiation and early development of an immune response enhances the production of Th2-type cytokines (IL-4 and IL-10) and inhibits Th1 cytokine, IFN-γ. Furthermore, treatment with soluble TIM-2 delays the development of EAE in SJL mice [49]. In TIM-2-deficient mice, lung inflammation is exacerbated in an obalbumin-induced airway hypersensitivity model, accompanied by dysregulated Th2 responses [50]. This phenotype is quite similar to that of Sema4A-deficient mice. Taken together, it is tempting to speculate that Sema4A–TIM-2 interaction negatively regulates of Th2

responses. However, there are some inconsistencies between these mutant mice (e.g., T cells from TIM-2-deficient mice but not from Sema4A-deficient mice show enhanced basal proliferation), which raises the possibility that Sema4A and/or TIM-2 have other binding partners. Indeed, T cells express some plexin-B family members and plexin-D1 to which Sema4A has binding activity [11].

Sema7A

Sema7A and Sema7A Receptors

Unlike other semaphorins, Sema7A/CD108 is a GPI-anchored protein. Sema7A transcripts are abundantly detected in adult tissues, including the brain, spinal cord, lung, testis, thymus and spleen [51, 52]. In the hematopoietic cells, Sema7A is expressed on erythrocytes and is also known as the John–Milton–Hagen human blood group anigen. In the immune system, Sema7A is predominantly expressed in $CD4^+CD8^+$ thymocytes and activated T cells [52].

Plexin-C1 was initially identified as a receptor for Sema7A [53]. Although the signal transduction pathways that transduce semaphoring–plexin-C1 functions remain largely unknown, plexin-C1 activation by Sema7A decreases integrin-mediated cell attachment and spreading [54]. Notably, however, Sema7A contains an arginine-glysine-asparate (RGD) sequence, a well-conserved integrin-binding motif. Indeed, Sema7A binds β1-integrins to induce axon outgrowth and contributes to lateral olfactory tract formation in the nervous system [55]. Furthermore, Sema7A–β1-integrin interactions promote melanocyte adhesion [54]. Therefore, it seems that Sema7A has opposing roles in regulating cell morphology and adhesion by binding different receptors.

Sema7A is an Initiator of Inflammatory Responses

In the immune system, Sema7A expressed by activated T cells stimulates macrophages to produce proinflammatory cytokines through the α1β1 integrin, also known as very late antigen 1 [56]. Recombinant soluble Sema7A stimulates macrophages to release peroxidase and produce proinflammatory cytokine, including IL-1β, IL-6, and TNFα. Furthermore, soluble Sema7A has much greater potency as a monocyte chemoattractant than canonical chemokines [57]. Sema7A induces phosphorylation of focal adhesion kinase, a direct downstream target of integrin signaling. Inflammatory cytokine production is significantly decreased in coculture of Sema7A-deficient T cell and wild-type macrophages, as well as in coculture of wild-type T cells and integrin α1-deficient macrophages [56]. Another Sema7A receptor plexin-C1 is also expressed in macrophages; however, soluble Sema7A-induced proinflammatory cytokine production is unaffected in macrophages from plexin-C1-deficient mice (unpublished data). Therefore, at least for the T cell–macrophage interactions, α1β1 integrin seems to be the predominant receptor for Sema7A.

In the later phase of T-cell-mediated immunity, antigen-specific effector T cells trigger inflammatory responses by activating macrophages in peripheral tissues. Both secreted and cell-associated factors from effector T cells [e.g., IFN-γ and CD40 ligand (CD40L), respectively] promote macrophage activation, which eliminates of pathogen at the infection focus, and can also lead to tissue destruction in autoimmune or allergic diseases. As a GPI-anchored protein, Sema7A is recruited to lipid rafts that accumulate at the immunological synapse between T cell and macrophage. At the lipid raft, Sema7A interacts with α1β1 integrin. Direct immunization of Sema7A-deficient mice and adoptive transfer of antigen-specific Sema7A-deficient T cells fails to induce T-cell-mediated immune responses such as contact hypersensitivity responses and EAE. Therefore, the interaction of Sema7A with α1β1 integrin is crucial for T-cell-mediated macrophage activation at sites of inflammation (Fig. 2c).

Thus far, IFN-γ and CD40L are the most potent T-cell effector molecules for promoting inflammatory responses in macrophages. However, these molecules require de novo synthesis after antigen recognition by macrophages. Furthermore, expression of CD40 on macrophages requires IFN-γ stimulation [58]. Given that Sema7A directly stimulates macrophages to produce proinflammatory cytokines, it is conceivable that Sema7A is involved in T-cell-macrophage concomitant activation and helps to initiate the inflammatory cascade.

Sema6D

Sema6D–plexin-A1 Interaction in Cardiac Development

Plexin-As are receptors for class III and VI semaphorins. Sema3A is a secreted semaphorin that binds to Nrp-1 to form receptor complex with plexin-A1 and transduce a repulsive axon guidance signal. On the other hand, Sema6D directly binds to plexin-A1 and exerts multiple biological effects. Both Sema6D and plexin-A1 are abundantly expressed in embryonic and adult tissues. Accumulating evidence has revealed a unique and complicated mechanism of Sema6D–plexin-A1 interaction during cardiac development. Ectopic Sema6D expression in chick embryo induces ventricular expansion with a decreased density of trabeculae. By contrast, knockdown of Sema6D results in

distorted bending of the cardiac tube. Sema6D inhibits the migration of ventricular endocardial cells but conversely enhances the migration of cells in the conotruncus region. Knockdown of plexin-A1 restores these defects to normal, suggesting that Sema6D–plexin-A1 interaction is crucial for cardiac development. Plexin-A1 forms a receptor complex with VEGFR2 in the conotruncal segment and with Otk (PTK7) in the ventricle segment to exert distinct biological effects [18]. Furthermore, Sema6D–plexin-A1 binding triggers the recruitment of activated tyrosine kinase Abl to the cytoplasmic domain of Sema6D during cardiac ventricle development, suggesting a reverse signaling of Sema6D [59].

Sema6D–plexin-A1 in DCs and Osteoclasts

In the immune system, various lymphocyte populations express Sema6D, including T, B, and NK cells. Plexin-A1 is one of the gene products induced by MHC class II transactivator, a master coactivator of MHC class II genes expressed in DCs, indicating that Sema6D–plexin-A1 engagement might be involved in T cell–DC interaction [60].

Production of IL-12 and expression of MHC class II are increased in DCs stimulated with recombinant soluble Sema6D although not in plexin-A1-deficient DCs. In addition, knockdown of plexin-A1 in DCs decreases the ability to prime T cells. Consistently, T-cell-mediated immunity is severely impaired in plexin-A1-deficient mice. These mice are resistant to MOG-induced EAE because of the defective generation of MOG-specific T cells [61]. These observations suggest that Sema6D on T cells stimulate DCs through plexin-A1, and this interaction is required for the efficient generation of antigen-specific T cells.

Plexin-A1 can associate with a variety of molecules to transduce intracellular signals. Recent study has identified that the triggering receptor expressed on myeloid cell-2 (TREM-2)-DAP12 complex associate with plexin-A1 in DCs and osteoclasts [61]. DAP12, a transmembrane adapter protein well known for its role in transducing activation signals, contains an immunoreceptor tyrosine-based activation motif in its cytoplasmic tail and recruits Src-like tyrosine kinases such as ZAP-70 and Syk. DAP12 is expressed in immune cells, such as NK cells and myeloid cells, and in osteoclasts and oligodendrocytes. Killer activity and ability of T-cell priming ability is decreased in DAP12-deficient NK cells and DCs, respectively [62, 63]. Furthermore, DAP12-deficient mice develop osteopetrosis and hypomyelinosis [64, 65]. Genetic mutations of human DAP12 result in a syndrome characterized by bone cysts and presentile dementia called Nasu–Hakola disease, also known as polycystic lipomembranous osteodysplasia with sclerosing leukoencephalopathy. Interestingly, plexin-A1-deficient mice also develop severe osteopetrosis due to impaired osteoclastogenesis [61]. The similarity of DAP12-deficient mice and plexin-A1-deficient mice phenotypes indicates that DAP12 might mediate plexin-A1 signaling in both DCs and osteoclasts (Fig. 2b).

Sema6D and Late Phase T-Cell Responses

Recently, O'Connor et al. [66] reported that Sema6D is highly detectable in $CD4^+$ T cells activated for 4 days. Blocking the Sema6D–Sema6D-ligand interaction by monoclonal antibody or recombinant soluble Sema6D protein decreases late-phase proliferation and CD127 induction of $CD4^+$ T cells. Although the interaction partner for Sema6D at the late phase of T cells is unknown, Sema6D on $CD4^+$ T cells may accelerate late phase T-cell responses.

Other Semaphorins and Semaphorin Receptors

Virus-Encoded Semaphorins

Viruses encode proteins in their own genomes that facilitate their transmission. Vaccinia virus semaphorin A39R/SemaVA, which only contains a small truncated extracellular sema domain, binds to plexin-C1 and induces aggregation, cytokine production, and surface expression of ICAM-1 (CD54) in human monocytes [67]. In addition, A39R suppresses integrin-mediated adhesion and migration of DCs and monocytes toward virus-infected cells [68]. A39R also interferes with phagocytosis by DCs [69]. Therefore, viral semaphorins might prevent DCs from acquiring antigens and/or suppress DC migration to lymph nodes to suppress immune cell function and provide a means for viruses to evade immune surveillance by suppressing immune cell functions.

Sema3A and its Immunosuppressive Roles

Sema3A was the first identified vertebrate semaphorin; its function as an axon repellent has been well established. Sema3A directly binds to Nrp-1, which induces activation of plexin-A1 and transduction of axon repulsive signals. Biological activity of Sema3A in the immune system has also been described. Consistent with its chemorepulsive effect on neurons, Sema3A inhibits spontaneous monocyte migration in vitro. Sema3A is expressed in activated DCs, T cells and some tumor cells and suppresses T-cell proliferation by inhibiting actin cytoskeletal reorganization and downregulating mitogen-activated protein kinases signaling [70]. Sema3A stimulation induces Fas transloca-

tion into lipid rafts and sensitizes Fas-mediated apoptosis in leukemic cells [71]. Moreover, Sema3A-deficient T cells exhibit enhanced proliferative responses to anti-CD3 [72]. These observations suggest that Sema3A serves as a negative regulator of T cells through autocrine/paracrine signaling.

Plexin-A4, a Candidate Receptor for Sema3A in the Immune System

Similar to other plexin A members, Plexin-A4 forms a receptor complex with Nrp1 to transduce class III semaphorin-mediated signaling. Plexin-A4 also directly binds to Sema6A [73]. Of the various immune cells, T cells, DCs, and macrophages, but not B and NK cells, express plexin-A4 transcripts. T-cell priming is enhanced, and EAE is exacerbated in plexin-A4-deficient mice. Hyperproliferation and enhanced TCR signals upon anti-CD3 stimulation are observed in plexin-A4-deficient T cells, comparable to that in Sema3A-deficient T cells [72]. Sema6A deficiency does not affect T-cell proliferation (unpublished data); therefore, it is tempting to speculate that Sema3A might be a major ligand for plexin-A4 in the immune system and that system negatively regulates T-cell responses. However, the detailed molecular mechanisms through which plexin-A4 regulates T cells and the relevance of other plexin-A members require further investigation.

Nrp-1/CD304 and Regulatory T Cells

Nrp-1 was originally described as a cell surface glycoprotein that acts as a class III semaphorin receptor, as described above. Nrp-1 is also known as human dendritic cell-specific antigen (blood dendritic cell antigen)-4, a specific plasmacytoid DC marker in humans and was assigned a CD number 304 in 2004. Nrp-1 is detectable in conventional mouse DCs. Tordjman et al. [74] first determined in the immune system that Nrp-1 is expressed in DCs and T cells and is involved in the initiation of primary immune responses. They showed that Nrp-1 localizes into the contact sites between T cells and DCs and proposed that Nrp-1 acts through a homophilic interaction. Later, Nrp-1 was identified as a specific marker for $CD4^+CD25^+$ regulatory T (Treg) cells [75]. Nrp-1 is part of the group of Foxp3-inducible genes, including CD25, GITR, and CTLA-4 [76]. The biological function of Nrp-1 in Treg cells has recently been described. Sarris et al. [77] revealed that Nrp-1 in Treg cells contributes to the long contact between Treg cells and DCs compared to the contact between naive T cells and DCs. Treg cells make stable contact with DCs that precede the contact of naive T cells with DCs, which might lead to the inhibition of T-cell activation in the steady state. Nrp-1-transduced naive T cells are endowed with the ability to have long interactions with DCs that are comparable to those between Treg cells and DCs [77]. However, whether the long contact is mediated by a homophilic interaction, or by semaphorins and Nrp-1 or Nrp-1-associating molecules such as plexins, remains to be elucidated.

Concluding Remarks

Accumulating evidence reveals that several semaphorins and their receptors have distinct biological activities in various phases of the immune responses ([78–80], see Table 1).

Table 1 Immune Semaphorins and their Functions

Class	Semaphorins	Expression in the immune system	Receptor	Receptor-mediated activity	References
III	3A	T, DC (activated)	Nrp-1-plexin-A1	Monocyte migration↓	[78]
			Nrp-1-plexin-A4?	T cell activation↓	[70–72]
IV	4A	DC, T (activated), Th1	TIM-2	T cell activation↑	[20]
				Th1 differentiation↑(or Th2 ↓)	[42]
	4D	T (high), B, DC (low), platelet, NK	CD72	DC activation↑	[37]
				B cell activation↑	[25, 32]
				NK cell killing activity↑	[80]
				thrombosis↑	[79]
			Plexin-B1	T cell-mediated neuroinflammation↑	[41]
VI	6D	DC, CD4+ T (long-term activated) NK, osteoclast	Plexin-A1	DC activation↑	[61]
				Osteoclastogenesis↑	[61]
			Plexin-A1?	Late phase CD4+ T cell response↑	[66]
VII	7A	CD4+ CD8+ thymocyte, T (activated), NK	α1b1integrin	Macrophage/monocyte activation↑	[56, 57]
				Monocyte migration↑	[57]
VIII (Viral)	A39R		Plexin-C1	DC and monocyte migration↓	[68]
				DC phagocytosis↓	[69]